The Plant Cell, Vol. 27: 574–590, March 2015, www.plantcell.org © 2015 American Society of Plant Biologists. All rights reserved.

Cleavage of *INDOLE-3-ACETIC ACID INDUCIBLE28* mRNA by MicroRNA847 Upregulates Auxin Signaling to Modulate Cell Proliferation and Lateral Organ Growth in Arabidopsis

Jing-Jing Wang[a,b] and Hui-Shan Guo[a,1]

[a] State Key Laboratory of Plant Genomics and National Center for Plant Gene Research (Beijing), Institute of Microbiology, Beijing 100101, China

[b] University of the Chinese Academy of Sciences, Beijing 100049, China

ORCID ID: 0000-0002-3057-9303 (H.-S.G.)

MicroRNAs function in a range of developmental processes. Here, we demonstrate that miR847 targets the mRNA of the auxin/indole acetic acid (Aux/IAA) repressor-encoding gene *IAA28* for cleavage. The rapidly increased accumulation of miR847 in *Arabidopsis thaliana* coincided with reduced *IAA28* mRNA levels upon auxin treatment. This induction of miR847 by auxin was abolished in auxin receptor *tir1-1* and auxin-resistant *axr1-3* mutants. Further analysis demonstrates that miR847 functions as a positive regulator of auxin-mediated lateral organ development by cleaving *IAA28* mRNA. Importantly, the ectopic expression of miR847 increases the expression of cell cycle genes as well as the neoplastic activity of leaf cells, prolonging later-stage rosette leaf growth and producing leaves with serrated margins. Moreover, both miR847 and *IAA28* mRNAs are specifically expressed in marginal meristems of rosette leaves and lateral root initiation sites. Our data indicate that auxin-dependent induction of miR847 positively regulates meristematic competence by clearing *IAA28* mRNA to upregulate auxin signaling, thereby determining the duration of cell proliferation and lateral organ growth in Arabidopsis. *IAA28* mRNA encodes an Aux/IAA repressor protein, which is degraded through the proteasome in response to auxin. Altered signal sensitization to *IAA28* mRNA levels, together with targeted IAA28 degradation, ensures a robust signal derepression.

INTRODUCTION

MicroRNAs (miRNAs), a class of short (21 to 24 nucleotides) noncoding RNAs, are processed in the nucleus as duplexes (miRNA:miRNA*) from primary miRNA transcripts (or *MIRNA*) containing imperfect intramolecular stem loops. The mature guide-stranded miRNA mediates the sequence-specific, post-transcriptional repression of mRNA targets (Jones-Rhoades et al., 2006; Carthew and Sontheimer, 2009). Most plant miRNAs directly cleave their targets, although in one case, diminution of the target protein without a corresponding reduction in the target mRNA indicates that plant miRNAs can also inhibit productive translation (Aukerman and Sakai, 2003; Chen, 2004). A recent study revealed the endoplasmic reticulum as the site of miRNA-mediated translation repression in *Arabidopsis thaliana* (Li et al., 2013). Plant miRNAs function in a range of developmental processes, ensuring proper embryonic, vegetative, and floral development (Jones-Rhoades et al., 2006) as well as tolerance and responses to extrinsic stresses (Sunkar and Zhu, 2004; Sunkar et al., 2006; Kruszka et al., 2012).

In Arabidopsis, miR172, miR156, miR159, and miR824 play important roles in the floral transition by targeting transcripts of the *Apetala2*, *Squamosa-promoter Binding Protein-Like*, *MYB* transcription factor, and *Agamous-Like16* genes (Park et al., 2002; Aukerman and Sakai, 2003; Achard et al., 2004; Chen, 2004; Schwab et al., 2005; Wang et al., 2009; Wu et al., 2009; Kim et al., 2012; Hu et al., 2014). miR165/166 and miR319 regulate leaf development and morphogenesis by targeting gene transcripts encoding HD-ZIP and TCP transcription factors, respectively (Reinhart et al., 2002; Rhoades et al., 2002; Palatnik et al., 2003; Tang et al., 2003; Juarez et al., 2004). miR160, miR167, and miR390 play roles in root and lateral root development, as well as embryo, leaf, and floral organ development, by targeting transcripts of *Auxin Response Factor10* (*ARF10*)/*ARF16*/*ARF17*, *ARF6*/*ARF8*, and *ARF2*/*ARF3*/*ARF4* genes, respectively (Mallory et al., 2005; Wang et al., 2005; Wu et al., 2006; Gutierrez et al., 2009; Liu et al., 2010; Marin et al., 2010; Yoon et al., 2010). While miR160 and miR167 directly target their *ARF* transcripts, miR390 targets *Trans-Acting siRNA3* to trigger the biogenesis of *trans*-acting small interfering RNAs, which subsequently inhibit ARF2/ARF3/ARF4 to release the repression of lateral root growth (Marin et al., 2010; Yoon et al., 2010). One miRNA may regulate multiple aspects of plant growth and development by targeting different mRNAs or interacting with other miRNA/target and environmental factors. For instance, targets of miR164 include mRNAs encoding five members of the NAC domain transcription factor family, including *NAC1*, *Cup-Shaped Cotyledon1* (*CUC1*), and *CUC2*. The expression of miR164 in root targets *NAC1* mRNA for cleavage to downregulate auxin signals for lateral root development (Guo et al., 2005), whereas the expression of miR164 in inflorescences targets *CUC1/2* to regulate the establishment and maintenance of the shoot apical and axillary meristems and floral boundary formation (Laufs et al., 2004; Mallory et al., 2004;

[1] Address correspondence to guohs@im.ac.cn.
The author responsible for distribution of materials integral to the findings presented in this article in accordance with the policy described in the Instructions for Authors (www.plantcell.org) is: Hui-Shan Guo (guohs@im.ac.cn).
www.plantcell.org/cgi/doi/10.1105/tpc.15.00101

Baker et al., 2005). A recent study shows that miR156 also functions antagonistically with miR171 in regulating trichome distribution in Arabidopsis (Xue et al., 2014).

Auxin signaling plays diverse and pivotal roles in many aspects of the growth and development of plants. ARFs are repressed by AUXIN/INDOLE ACETIC ACID (Aux/IAA) proteins, which are degraded through the proteasome mediated by the auxin receptor TRANSPORT INHIBITOR RESPONSE1 (TIR1) protein in response to auxin (Dharmasiri et al., 2005a, 2005b). The degradation of Aux/IAA releases the ARFs that bind to the auxin-responsive *cis*-acting element in early auxin response genes, including Aux/IAAs, small auxin-up RNAs, and a group of GH3 proteins identified as early auxin-responsive proteins (Hagen and Guilfoyle, 2002). Several *GH3* family genes mediate auxin homeostasis by conjugating amino acids to indole-3-acetic acid (Staswick et al., 2005) and further regulate root development (Guilfoyle and Hagen, 2007). In addition to repression by Aux/IAAs, the expression of many *ARFs* is directly mediated by at least one miRNA, such as miR160, miR167, or miR390 (Wang et al., 2005; Gutierrez et al., 2009; Marin et al., 2010; Yoon et al., 2010). miR393 also suppresses auxin signaling by degrading *TIR1* mRNA (Navarro et al., 2006). NAC1 acts downstream of TIR1 to transmit auxin signals (Xie et al., 2000), whereas miR164 induced by auxin downregulates auxin signals by clearing *NAC1* mRNA (Guo et al., 2005). These findings suggest that many miRNAs are involved in the response of plant hormones, particularly auxin, in the regulation of plant growth and development. However, the networks involving miRNA, mRNA, and plant hormones remain elusive.

Despite considerable research surveying the miRNA repertoire of individual plant species and the thousands of miRNAs in a diversity of plant species that have been predicted in the past decades (miRBase databases; http://mirbase.org), experimental functional studies of plant miRNAs are rather limited; as described above, most of these studies were confined to the abundant, previously identified, conserved miRNAs (Rajagopalan et al., 2006). Only a few low-abundance miRNAs, such as miR395 and miR399, have been studied in plants subjected to abiotic stresses (Jones-Rhoades and Bartel, 2004; Fujii et al., 2005; Chiou et al., 2006).

We report here a functional study of a low-abundance miRNA, miR847, in Arabidopsis. We found that the accumulation levels of miR847, which was not detected under normal circumstances, increased with decreasing *IAA28* mRNA levels upon auxin treatment. We confirmed the miR847-mediated cleavage of *IAA28* mRNA in vivo. IAA28, an Aux/IAA repressor, represses the auxin-induced transcription of genes that promote lateral root initiation (Rogg et al., 2001). We found that both miR847 and *IAA28* mRNAs have similar expression patterns and striking cell type specificity not only in the roots but also in the aerial portions of Arabidopsis. Analysis of transgenic plants overexpressing miR847 or *IAA28* cDNA and the *IAA28* knockout *iaa28-ko* mutant and the gain-of-function *iaa28-1* mutant revealed that the miR847/*IAA28* module regulates the extent of cell competence, thereby determining the duration of cell proliferation and the development of lateral organs, including lateral roots, rosette leaves, and axillary shoots in Arabidopsis.

RESULTS

Identification and Expression Profile of miR847

The function of miR847, which accumulates at low levels and was mainly isolated from Arabidopsis (Columbia-0 [Col-0] ecotype) seedlings (with 45 reads in a small RNA library containing 887,266 reads and 2, 2, and 5 reads in rosette leaves, flowers, and siliques, respectively) (Rajagopalan et al., 2006), was investigated. The accumulation of miR847 was undetectable in 8-d-old seedlings and roots and 2-week-old leaves, flowers, and siliques (Figure 1), whereas the accumulation of miR159 was readily detected (Figure 1A), consistent with the high cloning frequency of up to 6621 (for miR159a) and 982 (for miR159b) reads in the same small RNA library (Rajagopalan et al., 2006); these results confirm the low accumulation level of miR847. To determine the expression profile of the miR847-coding gene, we generated transgenic plants carrying a fusion of the precursor miR847 (*MIR847*) promoter and the β-glucuronidase gene (*GUS*). The expression of *MIR847-GUS* was readily detected in the shoot apex, leaf veins of the cotyledons, marginal meristems (leaf tooth) of the rosette leaves, sepals, stamen, and lateral root initiation sites (Figure 1B), indicating that *MIR847* is expressed at higher levels but within specialized cells of different organs. We then examined the processing efficiency of mature miR847 production. The *MIR847* backbone sequence was cloned into a construct under the control of the 35S promoter, producing 35S-MIR847. As a control, the miR159a precursor *MIR159a*, which is effective in expressing artificial miRNAs (Duan et al., 2008), was used as a backbone for the construction and expression of artificial miR847 under the control of the 35S promoter, producing 35S-miR$_{159}$847 (Figure 1C). As shown in Figure 1D, miR847 was more highly produced from 35S-miR$_{159}$847 than from 35S-MIR847 when they were transiently expressed in *Nicotiana benthamiana* via *Agrobacterium tumefaciens* infiltration, indicating the low processing efficiency of mature miRNA from the precursor-miR847 backbone sequence. This result might also explain the previous finding that only a close heterogeneous variant of the perfect miRNA* without the two-nucleotide 3′ overhangs typical of the Dicer-like products was sequenced (Rajagopalan et al., 2006). Nevertheless, both the striking cell type specificities and low processing efficiency indicate the low accumulation of miR847 under normal conditions.

miR847-Mediated Cleavage of the Predicted Target *IAA28* mRNA

Putative targets for miR847 were predicted through computational approaches (Wu et al., 2012). Plenty of potential targets were predicted (Supplemental Data Set 1). Dozens of sequences of the best putative targets, which had scores of 2.2 or 2.5, were examined by 5′ rapid amplification of cDNA ends (RACE). No cleavage fragments corresponding to predicted targets were obtained, presumably due to the low expression of miR847. Therefore, we transformed the above 35S-miR$_{159}$847 into wild-type Arabidopsis (Col-0). Figure 2 shows that the accumulation of miR847 was readily detected in all of the individual *35S-miR$_{159}$847*

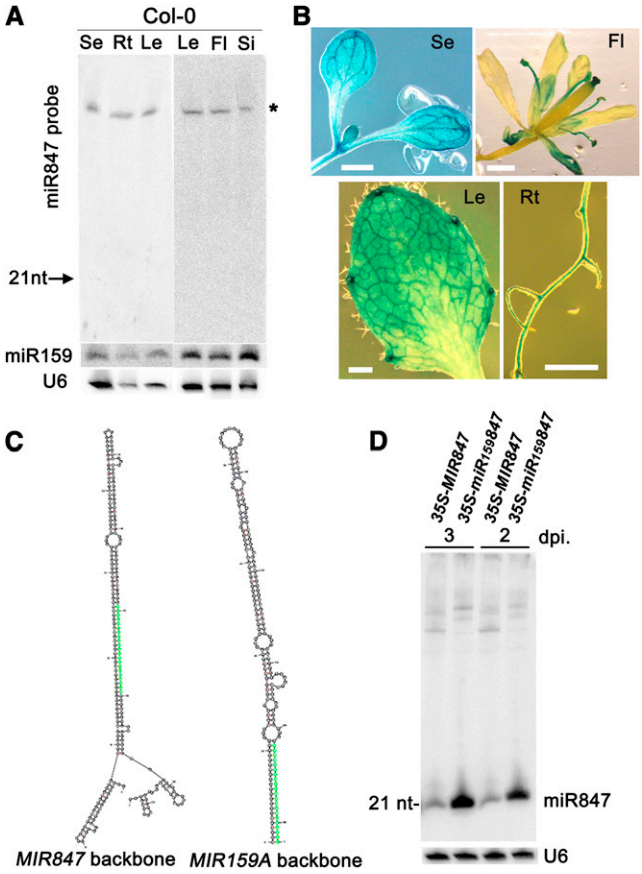

Figure 1. Expression Pattern of miR847.

(A) Examination of miR847 expression in various tissues of Arabidopsis. Small RNAs (60 μg, except 40 μg for roots) isolated from 8-d-old seedlings (Se), roots (Rt), and leaves (Le) and 2-week-old leaves, flowers (Fl), and siliques (Si) were loaded. LNA-modified oligonucleotide complementary to miR847 was used as a probe. No mature miR847 hybridization signal was detected. A band visible in the top blot (labeled with the asterisk) was possibly the miR847-coding precursor, *MIR847*, based on the size (230 bp) and detection by the miR847-specific sequence probe. The membrane was stripped and rehybridized with miR159-specific probe. The position of the miR159 hybridization signal in the original membrane is indicated by the arrow. U6 RNA hybridization is shown as a control.
(B) *MIR847-GUS* expression in 6-d-old seedling and 2-week-old leaf, root, and flower. Bars = 1 mm.
(C) Folding structure of *MIR847* and *MIR159A* backbones. Green highlighted nucleotides indicate the locations of mature miR847 and miR159.
(D) Detection of miR847 by transient expression of *35S-MIR847* and *35S-miR$_{159}$847* in *N. benthamiana*. Small RNAs (20 μg) isolated from *N. benthamiana* leaf at 2 and 3 d after infiltration (dpi) were used.

transgenic lines (Figure 2A). A 5′ RACE assay was performed, and a specific cleavage site within the miR847 complementary regions was obtained for only one potential target, *AT5G25890*, encoding *IAA28*, but not for any other predicted targets (Figure 2B). The cleaved site was at nucleotide 278 of the *IAA28* mRNA, which is located in, but not in the middle of, the miR847/*IAA28* mRNA complementary region. Consistent with the results of 5′ RACE, the accumulation level of *IAA28* was reduced consistently in 8-d-old seedlings and 25-d-old rosette leaves of different *35S-miR$_{159}$847* lines, as determined by RNA gel blot and quantitative RT-PCR (qRT-PCR) analyses (Figures 2A and 2C). There was no obvious change in the accumulation levels of other putative targets of miR847 in any of the *35S-miR$_{159}$847* lines tested (Figures 2A and 2C). To further confirm that the *IAA28* mRNA was the target of miR847, we introduced four nucleotide mutations into the miR847/*IAA28* mRNA complementary region of the *IAA28* mRNA sequence without changing the encoded amino acids, and the mutant (designated *IAA28m*) was confirmed to be resistant to miR847-mediated cleavage in a transient plant system assay (Figure 2D). Our results indicate that *IAA28* mRNA is a target of miR847.

miR847-Mediated Reduction of *IAA28* mRNA Levels upon Auxin Treatment

In a previous study, staining of 8-d-old transgenic Arabidopsis seedlings carrying a fusion of the *IAA28* promoter and the GUS gene showed promoter-GUS expression limited to roots (Rogg et al., 2001). *IAA28* mRNA was also concentrated in the roots and inflorescence stems, with minor levels in leaves and flowers (Rogg et al., 2001). To further examine whether the low level of *IAA28* in aerial portions of Arabidopsis was due to cell type specificities, as found for miR847, we first examined the expression profile of *IAA28* by generating *IAA28*-promoter-*GUS* (*IAA28-GUS*) transgenic Arabidopsis (Col-0). When 8-d-old seedlings were stained, *IAA28-GUS* was readily detected in roots but very weak in leaf veins of the cotyledons (Figure 3). However, staining of 12-d-old seedlings showed that *IAA28-GUS* was highly expressed in the shoot apex, leaf veins of the cotyledons, marginal meristems of the rosette leaves, sepals (but not stamens), and roots, especially at lateral root initiation sites (Figure 3A), revealing the striking cell type specificity and developmental regulation of *IAA28* expression. These expression patterns are similar to that of *MIR847*, suggesting that *IAA28* and miR847 function in the same types of cell.

IAA28 is a negative regulator of auxin signaling, and a reduction of *IAA28* mRNA was detected in response to auxin treatment (Rogg et al., 2001). To test whether the auxin-induced decrease in the *IAA28* mRNA level were mediated by miR847, the expression of miR847 in response to auxin treatment was examined. Ten-day-old wild-type Col-0 seedlings were treated with 1-naphthalene acetic acid (NAA) at 10 μM; we consistently detected an increase in miR847, but not in miR159a, at 2 h, and it reached the highest level at 4 h after treatment (Figure 3B). With 20 μM NAA treatment, the increase in miR847 was maintained at high levels for several hours (detected from 2 to 8 h after treatment), consistent with the increased expression of *GUS* transcript in *MIR847-GUS* transgenic plants upon auxin treatment (Supplemental Figure 1). Coincidently, reduced *IAA28* mRNA was detected from 2 h after auxin treatment, consistent with the detection of increased miR847 levels at 2 h (Figure 3C). Reduction of *IAA28* mRNA was not due to the decreased transcription of *IAA28* mRNA, because no change was detected in the expression of *GUS* in *IAA28-GUS* transgenic plants upon auxin treatment (Supplemental Figure 1). To confirm that *IAA28* is a direct target of miR847, transgenic *P$_{CsVMV}$-IAA28m* plants

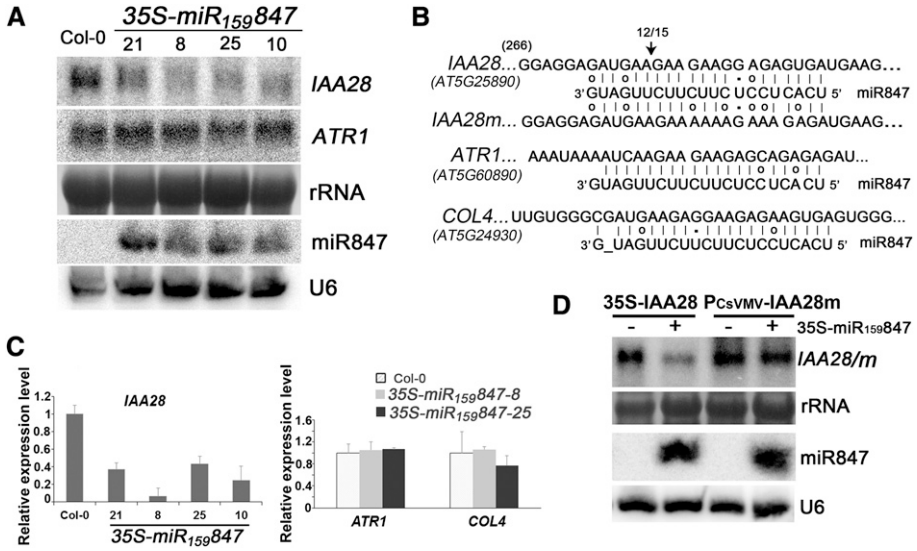

Figure 2. Identification of miR847 Targets.

(A) Overexpression of miR847 and effect of miR847 on *IAA28* mRNA accumulation. Total RNAs (30 μg) or small RNAs (60 μg) from 8-d-old seedlings of *35S-miR$_{159}$847* transgenic Arabidopsis and control Col-0 were used. *IAA28* mRNA and *ATR1* mRNA, two computational predicted targets of miR847, as well as miR847 are indicated. 28S rRNA and U6 were used as loading controls.

(B) Alignments of miR847 with *IAA28* (wild type) and *IAA28* mutant (*IAA28m*) and *ATR1* and *COL4* mRNAs, two of the computationally predicted targets. G-U base pairing is shown with dots, and mismatches are indicated with circles. The arrow indicates the cleavage site between nucleotides 277 and 278 of the *IAA28* mRNA detected by 5′ RACE analysis. Fifteen clones were sequenced, and an identical 5′ end was detected in 12 clones. No cleavage site was detected in the other computationally predicted targets, including *ATR1* and *COL4* mRNAs.

(C) Expression of *IAA28*, *ATR1*, and *COL4* mRNAs in *35S-miR$_{159}$847* transgenic plants. Total RNAs isolated from leaves of 25-d-old plants were quantified by qRT-PCR and normalized with the corresponding input RNA and *EIF1a* (as the internal standard) levels. The value of *IAA28* mRNA in Col-0 was arbitrarily designated as 1. Error bars represent SD for three replicates.

(D) Effect of miR847 on *IAA28* and *IAA28m* transcripts in coinfiltration assays. Total RNAs (30 μg) or small RNAs (20 μg) isolated at 2 d after infiltration were used. 28S rRNA and U6 were used as loading controls. Similar results were obtained from two individual assays.

expressing the cleavage-resistant mutant *IAA28m* were created. Ten-day-old seedlings were treated with 20 μM NAA, and a reduction of *IAA28* mRNA, but not the mutant *IAA28m* mRNA, by auxin treatment was observed (Figure 3C). Neither induction of miR847 nor reduction of *IAA28* mRNA levels by auxin was observed in the auxin-insensitive mutants *transport inhibitor response1* (*tir1-1*) and *auxin resistant1* (*axr1-3*) (Figures 3B and 3C). Taken together, our data indicate that the increase in the miR847 level is auxin-dependent, and the reduction in the *IAA28* mRNA level after auxin treatment resulted, at least in part, from miR847-mediated cleavage.

Transgenic Plants Overexpressing miR847 Promoted Lateral Root Initiation

IAA28 belongs to the Aux/IAA family and functions as an important component of the auxin signaling pathway implicated in lateral root initiation (De Rybel et al., 2010). A gain-of-function mutant, *iaa28-1*, strongly suppresses lateral root development in Arabidopsis Wassilewskija (Ws) (Rogg et al., 2001), revealing the negative effect of IAA28 on lateral root initiation (De Rybel et al., 2010). Therefore, the effect of miR847-mediated degradation of *IAA28* on lateral root development was examined in *35S-miR$_{159}$847* transgenic plants, an *IAA28* knockout line (SALK_129988C in Col-0; referred to *iaa28-ko* to distinguish it from the gain-of function *iaa28-1* in Ws), and wild-type Col-0. The overexpression of miR847 and the knockout of *IAA28* were hypothesized to result in more lateral roots. As expected, clear lateral roots were observed in 9-d-old seedlings of *35S-miR$_{159}$847* and *iaa28-ko* plants but were rarely found in Col-0 seedlings (Figure 4). Statistical analysis of the lateral root count per primary root in 5- and 6-d-old seedlings of *35S-miR$_{159}$847* lines, *iaa28-ko*, and Col-0 showed that the overexpression of miR847 or knockout of *IAA28* produced 2- to 3-fold more lateral roots than were present in the Col-0 controls (Figure 4B). Earlier and more lateral root development was conspicuous in 9- and 12-d-old *35S-miR$_{159}$847* and *iaa28-ko* seedlings (Figure 4A). By contrast, 9- and 12-d-old seedlings of *35S-IAA28-1* and *P$_{CsVMV}$-IAA28m* expressing the natural or the cleavage-resistant mutant *IAA28* mRNA (Figure 4A) developed fewer lateral roots compared with Col-0 control seedlings (Figure 4A), consistent with the opposite levels of accumulation of *IAA28* mRNA in *35S-IAA28* transgenic and *iaa28-ko* mutant plants. Similarly, fewer lateral roots were observed in the gain-of-function *iaa28-1* mutant compared with Ws control seedlings (Supplemental Figure 2). There was no significant difference in lateral root development between seedlings of *35S-IAA28* and *P$_{CsVMV}$-IAA28m*, presumably because there was no substantial difference between

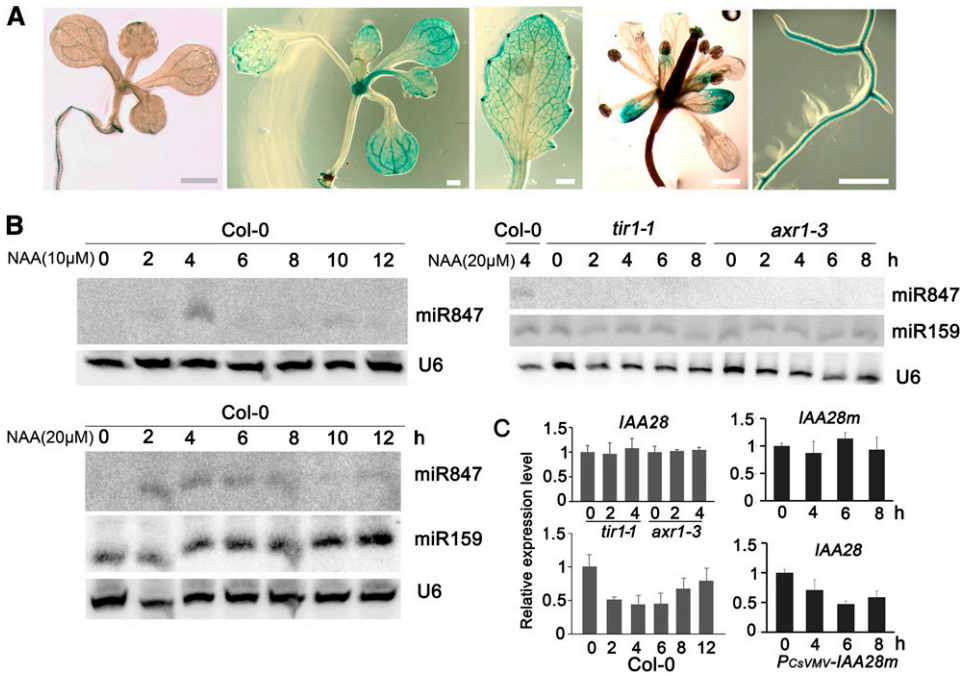

Figure 3. Expression Pattern of IAA28 and Its Reduction Coincident with the Induction of miR847 upon Auxin Treatment.

(A) *IAA28-GUS* expression in 8- or 12-d-old seedling, leaves, flower, and root. Bars = 1 mm.

(B) Induced expression of miR847 upon auxin treatment. Ten-day-old wild-type Col-0 and *tir1-1* and *axr1-3* mutant seedlings were treated with 10 or 20 μM NAA, and samples were collected at the times indicated at top. Eighty micrograms of small RNA samples was loaded for hybridization with miR847 LNA probe. miR159 and U6 hybridization was used as controls.

(C) Reduced expression of *IAA28*, but not *IAA28m*, upon auxin treatment. Total RNAs were isolated from 10-d-old Col-0, P_{CsVMV}-*IAA28m*, and *tir1* and *axr1-3* mutant seedlings treated with 20 μM NAA at the indicated time points. The expression of *IAA28* or *IAA28m* was quantified by qRT-PCR amplified with sequence-specific primers (Supplemental Data Set 2) and normalized with the corresponding input RNA and *UBQ10* (as the internal standard) levels. The value of *IAA28* or *IAA28m* mRNA at 0 h was arbitrarily designated as 1. Error bars represent SD for three replicates.

wild-type and mutant *IAA28* mRNAs at the low-abundance level of miR847 under normal conditions.

Previous studies demonstrated that an IAA28-dependent auxin signaling mechanism in the basal meristem regulates the expression of the transcription factor gene *GATA23*, which determines lateral root founder cell identity (De Rybel et al., 2010). Therefore, we examined the expression of *GATA23* mRNA in the above plants of various genotypes (the *35S-miR*$_{159}$*847*, *iaa28-ko*, *35S-IAA28-1*, and P_{CsVMV}-*IAA28m* lines). A qRT-PCR analysis demonstrated that the expression level of *GATA23* mRNA was remarkably increased in the roots of 8-d-old *35S-miR*$_{159}$*847* and *iaa28-ko* seedlings compared with the Col-0 control (Figure 4C). Plants of the *35S-miR*$_{159}$*847* line (line 8), with a lower level of *IAA28* mRNA (Figure 2C), accumulated higher levels of *GATA23* mRNA (Figure 4C), consistent with greater lateral root formation (Figure 4A). In contrast, decreased levels of *GATA23* mRNA were detected in the roots of *35S-IAA28-1* and P_{CsVMV}-*IAA28m* seedlings (Figure 4C). To determine whether the production of more lateral roots in *35S-miR*$_{159}$*847* plants possibly involved other factors that also affect lateral root development, the expression of transcription factor *NAC1*, which transduces auxin signals for lateral root emergence (Xie et al., 2000; Guo et al., 2005), was examined. A qRT-PCR analysis showed no difference in the expression levels of *NAC1* mRNA between the roots of 8-d-old seedlings of the various genotypes and the Col-0 control (Figure 4C). Thus, our data indicate that greater lateral root development in *35S-miR*$_{159}$*847* seedlings presumably results from the miR847-mediated reduction of *IAA28* mRNA and subsequent activation of *GATA23* to promote lateral root initiation.

Transgenic Plants Overexpressing miR847 Presented a Series of Abnormal Aerial Phenotypes Opposite to Those of Plants Overexpressing *IAA28* mRNA

In addition to greater lateral root development in the *35S-miR*$_{159}$*847* plants, we observed serial abnormal aerial phenotypes in these transgenic lines throughout plant growth. Because both miR847 and *IAA28* presented striking cell type specificities in aerial tissues (Figures 1 and 3) and the aerial portions of the gain-of-function *iaa28-1* mutant plants were also malformed (Rogg et al., 2001), we investigated the possible involvement of miR847 and IAA28 in the regulation of the development of the aerial part of Arabidopsis. We compared the aerial part phenotypes of the *35S-miR*$_{159}$*847*, *iaa28-ko*, and P_{CsVMV}-*IAA28m* plants as well as the wild-type Col-0. In 6- and 8-d-old seedlings, Col-0 developed normal oval cotyledons,

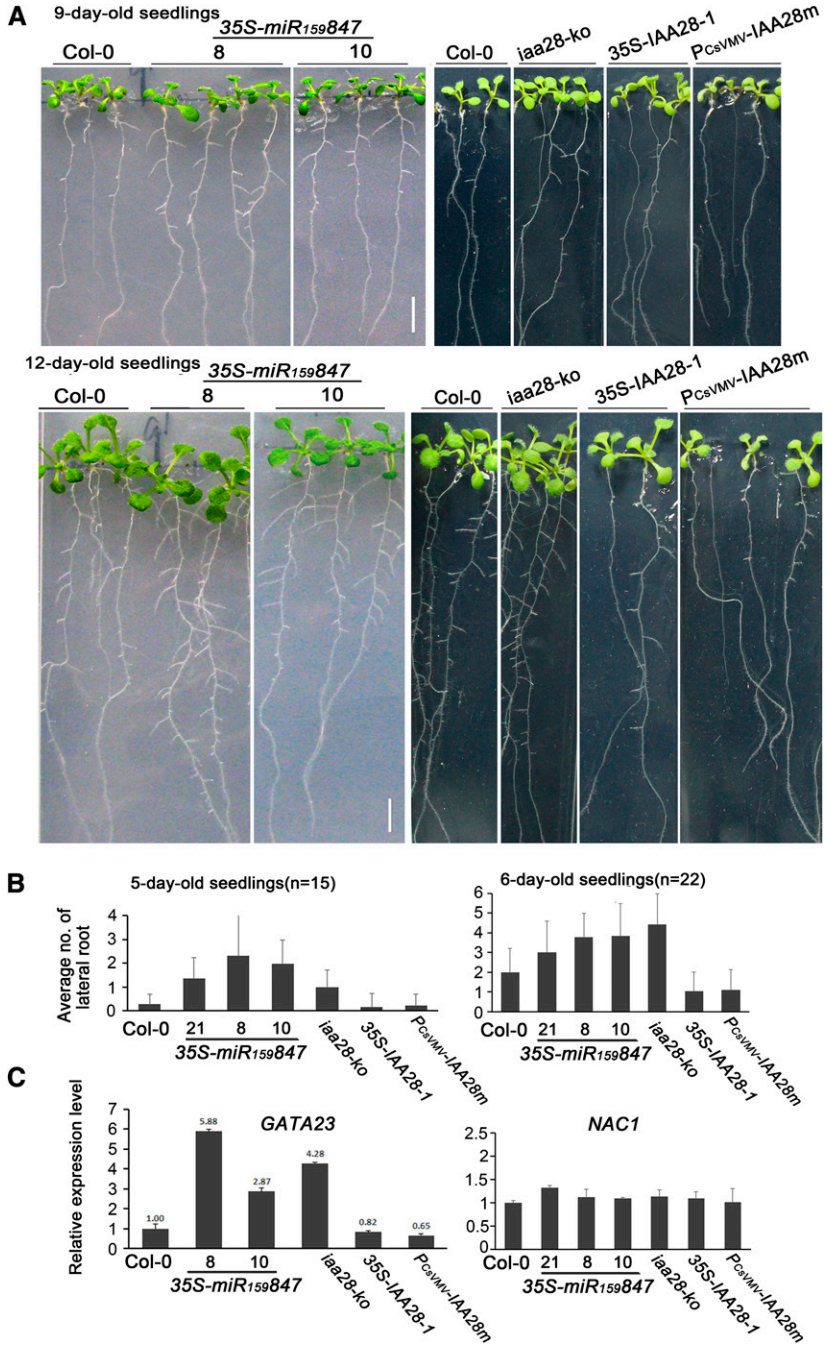

Figure 4. Effect of the Overexpression of miR847 on Lateral Root Development.

(A) Early and sustained formation of lateral roots in the *35S-miR$_{159}$847* transgenic lines. Col-0 and *35S-miR$_{159}$847*, *iaa28-ko*, *35S-IAA28-1*, and *P$_{CsVMV}$-IAA28m* seedlings were grown on MS medium with 3% sucrose. Seedlings were photographed at 9 and 12 DAG. Bars = 5 mm.

(B) Statistical histogram of the average number of lateral roots in 5- and 6-d-old seedlings of each genotype. Roots were observed with a binocular microscope to acquire numbers of lateral root initials identified by staining whole seedlings with a mixture of toluidine blue and basic fuchsin and then counted. The average number of lateral roots was obtained from 15 (n = 15) or 22 (n = 22) seedlings of each genotype. Error bars represent SD for the average number.

(C) Analysis of the expression of *GATA23* and *NAC1* mRNAs in 8-d-old roots. Total RNAs isolated from roots of each genotype were quantified by qRT-PCR and normalized with the corresponding input RNA and *ACTIN2* (as the internal standard) levels. The values of *GATA23* and *NAC1* mRNAs in Col-0 were arbitrarily designated as 1. Error bars represent SD for three replicates.

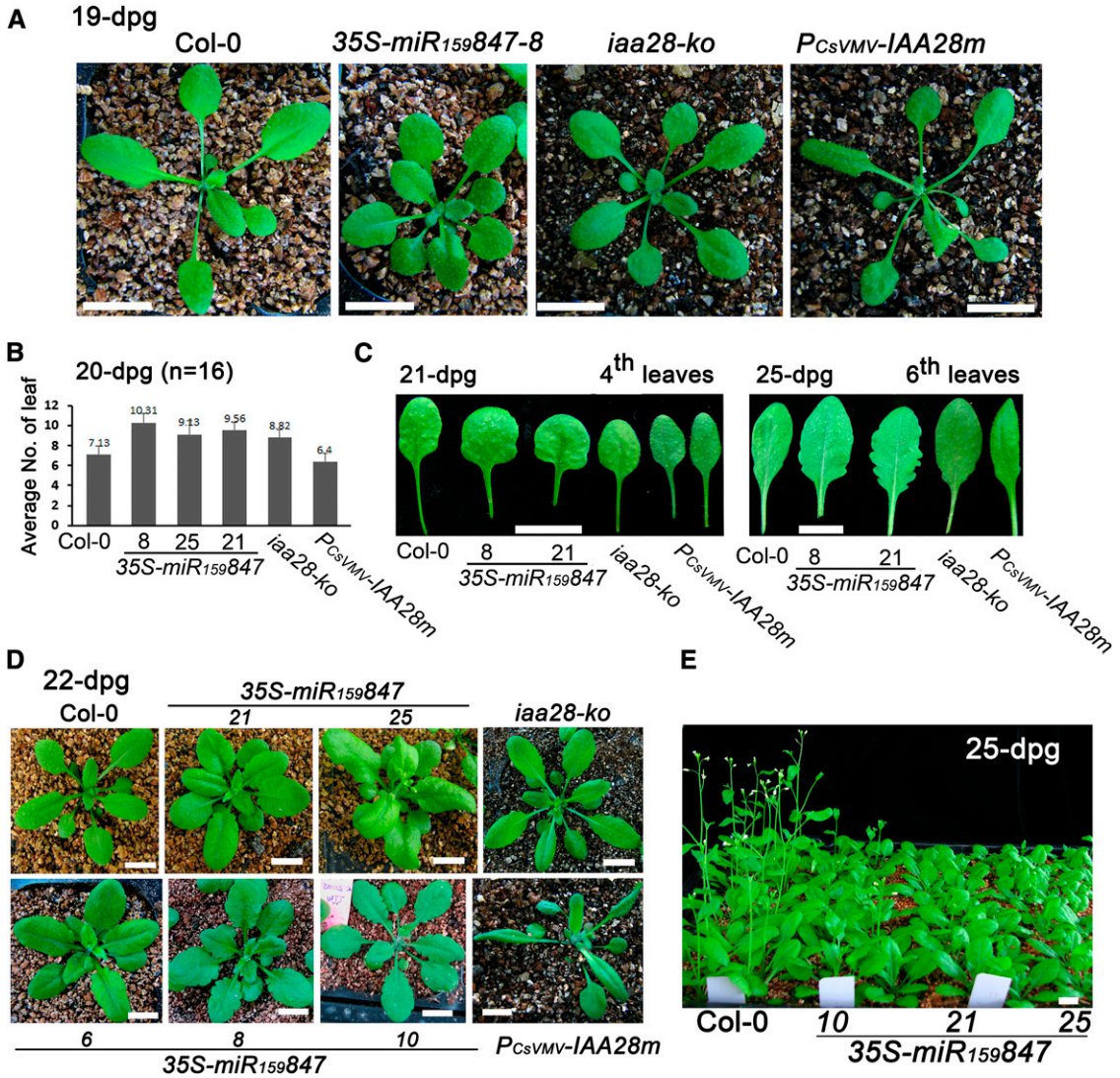

Figure 5. Phenotypes of *35S-miR$_{159}$847*and *P$_{CsVMV}$-IAA28m* Transgenic and *iaa28-ko* Mutant Plants.

(A) Developmental phenotypes of Col-0, *35S-miR$_{159}$847-8*, *iaa28-ko* mutant, and *P$_{CsVMV}$-IAA28m* plants at 19 DAG. Bars = 10 mm.
(B) Statistical histogram of the average number of leaves in Col-0, *35S-miR$_{159}$847* transgenic lines 8, 25, and 21, *iaa28-ko* mutant, and *P$_{CsVMV}$-IAA28m* plants at 20 DAG. Sixteen plants of each genotype were counted. Error bars represent SD for the average number.
(C) Leaf morphologies of Col-0, *35S-miR$_{159}$847* and *P$_{CsVMV}$-IAA28m* transgenic lines, and *iaa28-ko* mutant plants at 21 and 25 DAG. Bars = 5 mm.
(D) Representative phenotypes of various *35S-miR$_{159}$847* and *P$_{CsVMV}$-IAA28m* transgenic lines and *iaa28-ko* mutant plants. Bars = 10 mm.
(E) Floral development in Col-0 and *35S-miR$_{159}$847* transgenic lines at 25 DAG. Bar = 10 mm.

and round and/or slightly heart-shaped cotyledons were observed in the *35S-miR$_{159}$847* and *iaa28-ko* seedlings, while the *P$_{CsVMV}$-IAA28m* seedlings showed slightly longer oval cotyledons (Supplemental Figure 3). During the early development stage, *35S-miR$_{159}$847* and *iaa28-ko* seedlings were generally smaller, with shorter petioles, smaller leaf size, and shorter hypocotyls, compared with the Col-0 control, while the *P$_{CsVMV}$-IAA28m* seedlings presented an opposite phenotype, with longer petioles and hypocotyls (Supplemental Figure 3). Consistently, slightly longer petioles and hypocotyls in the gain-of-function mutant *iaa28-1* were also observed compared with wild-type Ws (Supplemental Figure 3). Throughout plant growth, the morphology of the *35S-miR$_{159}$847* plants appeared compact and leafy compared with that of Col-0 (Figure 5). At ~20 d after germination (DAG), 7 to 8 true leaves developed in the Col-0 plants and 9 to 11 leaves were consistently observed in the *35S-miR$_{159}$847*and *iaa28-ko* plants, whereas 6 to 7 leaves were observed in the *P$_{CsVMV}$-IAA28m* plants (Figures 5A and 5B). Inverse phenotypes were also observed in both the true leaf size and the morphology of the leaf margin between the *35S-miR$_{159}$847*, *iaa28-ko*, and *P$_{CsVMV}$-IAA28m* plants. The early developed leaves (e.g., 3rd and 4th true leaves) of the *35S-miR$_{159}$847* and *iaa28-ko*

plants were shorter and wider, but those of P_{CsVMV}-*IAA28m* were smaller than those of Col-0 (Figure 5C). Then, juvenile leaves (e.g., 6th to 10th true leaves) emerged that were larger in both *35S-miR$_{159}$847* and *iaa28-ko* plants compared with those in Col-0 (Figure 5C). Some of the *35S-miR$_{159}$847* plants had a notable serrated margin (Figure 5C). A strong serrated leaf margin was observed in 39 out of 63 primary *35S-miR$_{159}$847* transformants (Figure 5D). Leaves in similar layers were slender with a smooth margin in P_{CsVMV}-*IAA28m* plants (Figure 5C). The production of the floral organs was normally observed at 22 DAG in Col-0 but with a 3- to 5-d delay in the *35S-miR$_{159}$847* plants (Figure 5E).

The total leaf number and average fresh weight per plant were also compared among the *35S-IAA28*, *35S-miR$_{159}$847* transgenic, *iaa28-ko* mutant, and Col-0 plants. Plants of these genotypes that were 33 d old were used (Figure 6). The *35S-IAA28* plants had fewer rosette leaves and lower average fresh weights compared with the Col-0 plants (Figures 6B and 6D). The *35S-miR$_{159}$847* and *iaa28-ko* mutant plants produced more rosette

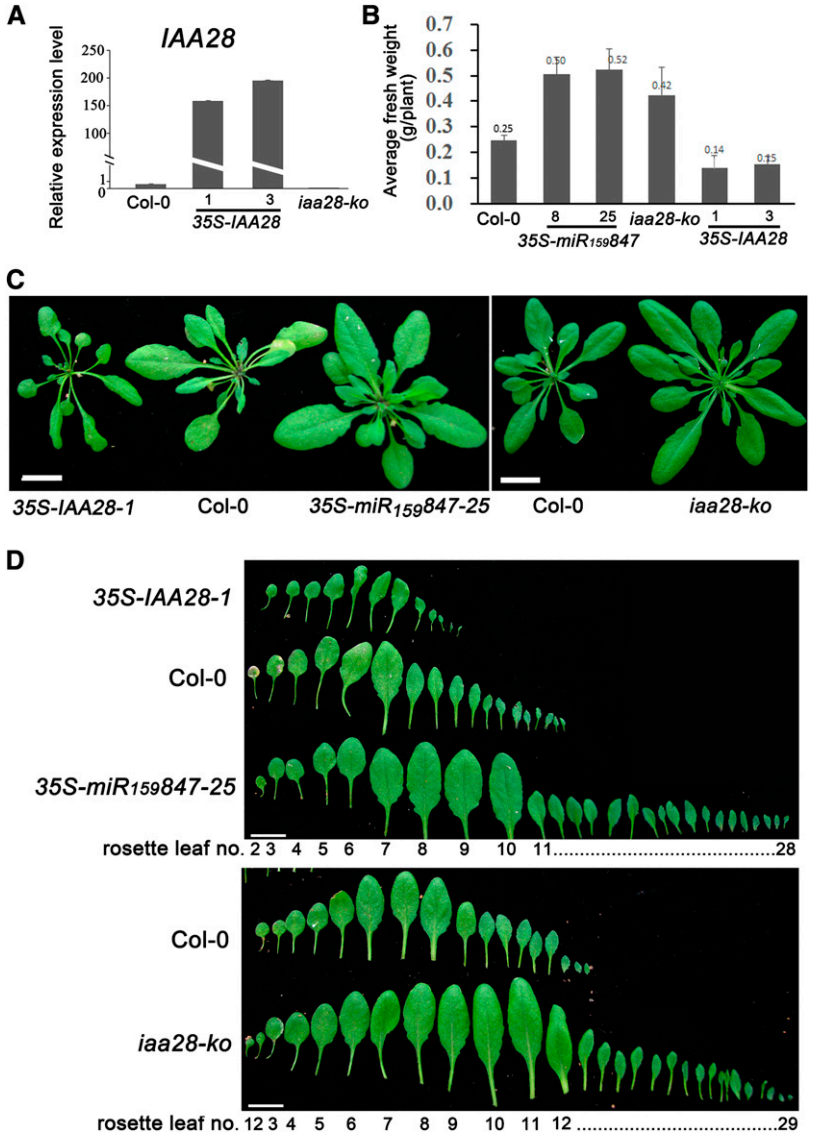

Figure 6. Plants Overexpressing the *IAA28* mRNA Display the Opposite Phenotype to That of *35S-miR$_{159}$847*.

(A) The expression of *IAA28* mRNA in Col-0, *35S-IAA28* transgenic, and *iaa28-ko* mutant plants at 33 DAG was quantified by qRT-PCR as described in Figure 2C.

(B) Average fresh weight of rosette leaves of Col-0, *35S-miR$_{159}$847*, *iaa28-ko*, and *35S-IAA28* transgenic plants at 33 DAG with inflorescences removed. Ten plants of each genotype were used. Error bars represent SD for the average number.

(C) and **(D)** Plants with inflorescences removed **(C)** and peeled off rosette leaves **(D)** of *35S-IAA28-1*, Col-0, *35S-miR$_{159}$847-25*, and *iaa28-ko* at 33 DAG. Bars = 10 mm.

leaves and had a remarkably increased average fresh weight compared with Col-0 (Figures 6B and 6D). The finding that the phenotypes of plants overexpressing miR847 resembled those of *iaa28-ko* plants and were opposite those of plants overexpressing *IAA28* mRNA reveals that miR847-mediated degradation of *IAA28* is involved in the regulation of aerial portion development.

Notably, a previous study reported that only transgenic plants overexpressing the gain-of-function mutant *iaa28-1* gene had severe defects, with an infertile dwarf phenotype, while overexpression of *IAA28* caused no discernible morphological effects (Rogg et al., 2001). In our *35S-IAA28* plants, slender and fewer leaves and advanced inflorescence were observed, but none of the *35S-IAA28* lines had extreme phenotypes of infertile dwarfs throughout the experimental periods (longer than 2 months). IAA28 was previously shown to have the longest (~80 min) half-life of the four canonical Aux/IAA proteins, as estimated using luciferase-fusing proteins (10 to 20 min for IAA1, IAA9, and IAA17) (Ramos et al., 2001; Dreher et al., 2006). We speculate that the different growth conditions and/or different product levels of the transgenic *IAA28* mRNA, in addition to the dramatically different half-life of IAA28 compared with other Aux/IAAs (Dreher et al., 2006), might cause the phenotypic discrepancies of transgenic plants overexpressing wild-type *IAA28* cDNA.

Overexpression of miR847 Downregulates the IAA28-Mediated Repression of Auxin Signaling in Aerial Portions

Because the miR847-mediated cleavage of *IAA28* mRNA resulted in the derepression of auxin signaling, leading to lateral root formation (Figure 4), we hypothesized that the opposite abnormal phenotypes observed in the aerial portions of the *35S-IAA28* and *35S-miR$_{159}$847* plants also resulted from the repression and derepression of auxin signaling in aerial portions of two genotypes. To determine which auxin regulation genes are possibly regulated by IAA28, several early auxin response genes of two major classes, *GH3* and *Aux/IAA*, were tested using samples from the aerial portions of 13-d-old seedlings. The accumulation levels of *GH3.5*, an auxin-responsive *GH3* gene also known as *WES1* (At4g27260), which encodes IAA-amide synthetases that help maintain auxin homeostasis (Staswick et al., 2005), but not *GH3.2*, were reduced in the *35S-IAA28* and *P$_{CsVMV}$-IAA28m* plants but increased in the *35S-miR$_{159}$847* and *iaa28-ko* mutant plants compared with Col-0 (Figure 7), consistent with a previous report that a light-grown *GH3.5* (*WES1*)-overexpressing *wes1-D* mutant developed short hypocotyls. By contrast, the knockout *wes1* mutant hypocotyls were slightly longer than the control Col-0 hypocotyls (Park et al., 2007). The expression of *IAA3*, a primary auxin response gene, was also reduced in *35S-IAA28* and *P$_{CsVMV}$-IAA28m* but increased in *35S-miR$_{159}$847* and *iaa28-ko* mutants compared with Col-0 plants, although the increased level in *iaa28-ko* was not as high as in *35S-miR$_{159}$847* (Figure 7A). This is consistent with the gain-of-function mutations in *IAA3* producing short hypocotyls (Tian et al., 2002). Our results suggest that the short hypocotyl auxin phenotype in *35S-miR$_{159}$847* plants (Figure 5) can probably be attributed to the increase in the expression of *GH3.5* and *IAA3* upon miR847-mediated downregulation of *IAA28.*

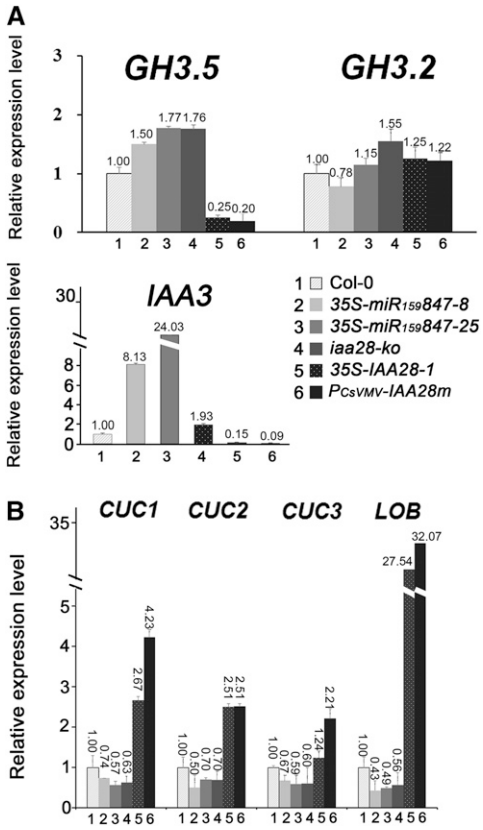

Figure 7. RNA Analysis of Early Auxin-Responsive and Auxin Signaling-Repressive Genes in *35S-miR$_{159}$847* Transgenic Plants.

The expression of early auxin response genes, *GH3.5*, *GH3.2*, and *IAA3* **(A)**, and auxin signaling-repressive genes, *CUC1*, *CUC2*, *CUC3*, and *LOB* **(B)**, is shown in Col-0, *35S-miR$_{159}$847* transgenic (lines 8 and 25), *iaa28-ko* mutant, and *35S-IAA28-1* and *P$_{CsVMV}$-IAA28m* plants. Total RNAs isolated from aerial parts of 13-d-old seedlings were quantified by qRT-PCR and normalized with the corresponding input RNA and *UBQ10* (as the internal standard) levels. The value of each mRNA in Col-0 was arbitrarily designated as 1. Error bars represent SD for three replicates.

The initiation of plant lateral organs from the shoot apical meristem (SAM) is associated with the formation of boundaries that separate the primordia from the surrounding tissue (Aida and Tasaka, 2006; Rast and Simon, 2008). We examined the *CUC* family genes, which are required for the activation of genes that maintain meristematic fate in the SAM and are negatively regulated by auxin-dependent signaling (Berleth et al., 2004; Laufs et al., 2004; Hibara et al., 2006; Rast and Simon, 2008), and *LATERAL ORGAN BOUNDARIES* (*LOB*) mRNA, which is expressed at the base of all lateral organs and mediates the response to auxin (Inukai et al., 2005; Okushima et al., 2007). In the aerial portions of 13-d-old seedlings, the accumulation of *CUC1*, *CUC2*, *CUC3*, and, especially, *LOB* mRNAs was reduced in *35S-miR$_{159}$847* and *iaa28-ko* mutant plants but increased in the *35S-IAA28* and *P$_{CsVMV}$-IAA28m* plants compared with Col-0 (Figure 7B). The induction was also prominent for *LOB*. The redundant functions of the *CUC1*, *CUC2*, and *CUC3* genes (Mallory et al., 2004; Shani et al., 2006) in the regulation of embryonic shoot

meristem formation and cotyledon boundary specification (Hibara et al., 2006) might account for the inconspicuous changes in transcript levels of *CUC* family genes and the slightly heart-shaped cotyledon phenotype in the *35S-miR$_{159}$847* seedlings (Supplemental Figure 3). Nonetheless, our findings suggest that the miR847-mediated degradation of *IAA28* increases auxin signaling, probably by decreasing the expression of *LOB* and *CUC* family genes to promote the initiation of leaf primordia and consequently increase the number of leaves.

Overexpression of miR847 Reduces *IAA28* mRNA Levels to Prolong Growth and Cell Proliferation

In addition to exhibiting an increased number of leaves, similar to the *iaa28-ko* mutant, *35S-miR$_{159}$847* plants also had remarkably increased leaf sizes of the 8th to 10th rosette leaves compared with those of Col-0, in which the leaves from the 8- to 9-leaf stage generally stopped growing after flowering (Figure 6). To determine whether the larger leaves were due to cell expansion or increased cell numbers, the 6th and 8th leaves of 33-d-old *35S-miR$_{159}$847-25* and Col-0 plants were selected for microscopic observation. In these two leaves, cells, especially the epidermal cells, in the *35S-miR$_{159}$847-25* plants were likely turgid, because the cell margin was less wrinkled compared with that in Col-0 (Figure 8), leading to the slightly larger size of both epidermal and mesophyll cells in the *35S-miR$_{159}$847-25* plants than in Col-0. Except for mesophyll cells in the 8th leaf, the number of cells in the same area of leaves was not much different between Col-0 and *35S-miR$_{159}$847-25*. The numbers of mesophyll cells in the same area in the 8th leaf of Col-0 was ~2.3-fold more than that of *35S-miR$_{159}$847-25* (Figure 8A), in agreement with the slightly larger size of mesophyll cells in the *35S-miR$_{159}$847-25* plants than in Col-0. However, this slightly larger size of the cells could not explain the at least four times larger 8th, 9th, and 10th leaves in *35S-miR$_{159}$847-25* plants compared with Col-0 (Figure 6D).

Because both *MIR847* and *IAA28* were expressed in the marginal meristems (leaf tooth) of the rosette leaves (Figures 1

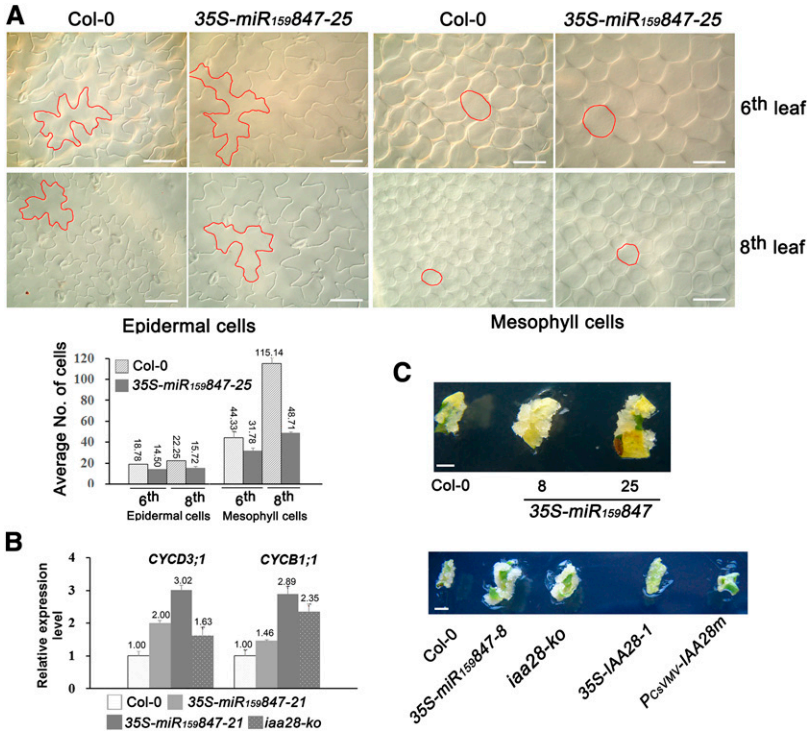

Figure 8. Ectopic Expression of miR847 Prolongs Growth and Cell Proliferation.

(A) Morphologies of adaxial epidermal cells and mesophyll cells of sixth and eighth leaves of Col-0 and *35S-miR$_{159}$847-25* plants at 33 DAG. Leaves were transparentized and observed using an HC/DMR microscope (Leica) equipped with Nomarski optics. One representative cell in each photograph is outlined in red. The average number of cells counted under the same magnification is indicated. Error bars represent SD for three views of each sample. Bars = 50 μm.

(B) The expression of *CYCD3;1* and *CYCB1;1* in 33-d-old rosette leaves of Col-0, *35S-miR$_{159}$847* transgenic (lines 21 and 25), and *iaa28-ko* plants was quantified by qRT-PCR and normalized with the corresponding input RNA and *AT3G33380* (as the internal standard) levels. Error bars represent SD for three replicates.

(C) Callus growth in leaf explants of Col-0, *35S-miR$_{159}$847* transgenic (lines 8 and 25), *iaa28-ko* mutant, and *35S-IAA28-1* and *P$_{CsVMV}$-IAA28m* transgenic plants. The explants were cultured on MS medium containing 100 ng/L 2,4-D and 100 ng/L 6-BA in the dark and photographed on day 7 without changing the medium. Bars = 2 mm.

and 3), where cells maintain meristematic competence, we investigated the involvement of miR847 and IAA28 in cell proliferation. Two genes that are involved in the cell cycle were examined. *CYCD3;1*, a G1 cyclin gene (Hu et al., 2000; Dewitte et al., 2003), and *CYCB1;1*, which is expressed during the G2/M phase of the cell cycle (Ferreira et al., 1994a, 1994b; Donnelly et al., 1999), were analyzed in 33-d-old rosette leaves of the *35S-miR$_{159}$847*, *iaa28-ko*, and Col-0 plants. The upregulation of the two mRNAs was detected in *35S-miR$_{159}$847* and *iaa28-ko* plants compared with Col-0 (Figure 8B), indicating that the ectopic expression of miR847 or knockout of *IAA28* increased the expression of *CYCD3;1* and *CYCB1;1* and sustained cell meristematic competence to prolong later-stage rosette leaf growth. Consistently, the leaves of the *35S-miR$_{159}$847* plants displayed strong serrations in the leaf blade, whereas smooth leaf blades were observed in the *IAA28*-overexpressed *P$_{CsVMV}$-IAA28m* plants (Figure 5C), suggesting the important regulatory roles of miR847/*IAA28* in marginal cell division during development. The opposite effects of miR847 and IAA28 on cell proliferation were further supported by the formation of callus during tissue culture. Leaf explants that were cultured on callus induction medium (with 2,4-D and 6-benzyl aminopurine [6-BA]) for 1 week produced larger calli for *35S-miR$_{159}$847* and *iaa28-ko* than for the Col-0 plants; by contrast, the leaf explants of the *35S-IAA28-1* and *P$_{CsVMV}$-IAA28m* plants produced almost no visible calli in 1 week (Figure 8C), and small calli from the *35S-IAA28-1* and *P$_{CsVMV}$-IAA28m* plant leaf explants were observed after 2 weeks, consistent with the high activity of IAA28 in repressing cell division during the auxin response. Taken together, our results indicate that the overexpression of miR847 downregulates *IAA28*, leading to prolonged growth and cell proliferation.

Overexpression of a Cleavage-Resistant Form of *IAA28* mRNA Rescues the Abnormal Developmental Morphologies of *35S-miR$_{159}$847* Transgenic Plants

To further demonstrate that the overexpression of miR847, leading to the downregulation of *IAA28*, is responsible for the abnormal development morphologies, we introduced the cleavage-resistant form of *IAA28m* mRNA into *35S-miR$_{159}$847* plants. The *35S-miR$_{159}$847* plants of line 8, which showed a strong abnormal phenotype, were retransformed with *P$_{CsVMV}$-IAA28m*, a construct harboring *IAA28m* under the control of the cassava vein mosaic virus (CsVMV) promoter, generating *IAA28m/miR847-8* transgenic plants. If miR847 targets *IAA28*, but not other computationally predicted endogenous genes, for cleavage, overexpression of cleavage-resistant *IAA28m* in *35S-miR$_{159}$847* plants would rescue its abnormal phenotypes. The accumulation of miR847 and the increased expression of *IAA28m* were confirmed in all retransformants (Figure 9). As expected, most of the *IAA28m/miR847-8* primary transformants (five out of seven lines, including line 3) likely rescued the abnormal development morphologies of *35S-miR$_{159}$847-8*, producing morphologies such as the normal length of the leaf petioles and hypocotyls, normal ovate cotyledons (Supplemental Figure 3), and leaf numbers and sizes that are similar to those of wild-type Col-0 (Figure 9A); these rescued phenotypes are consistent with the restoration of the expression levels of most of the tested auxin response genes, such as *GH3.5*, *CUC2*, *CUC3*, and *LOB* mRNAs, compared with that in Col-0 (Figure 9C). The expression levels of *IAA3* mRNA in the *IAA28m/miR847-8* plants were also remarkably reduced compared with those of the *35S-miR$_{159}$847-8* plants, but they were higher than those of Col-0 (Figure 9C), reflecting the complex roles of negative regulators in auxin signaling. Negative autoregulation has been demonstrated in an *IAA3* gain-of-function mutant (Tian et al., 2002). The high level of *IAA28m* in the *IAA28m/miR847-8* plants might account for this discrepancy. Indeed, two out of the seven *IAA28m*/miR847 lines (including line 2) with a high accumulation level of *IAA28m* mRNAs presented weak phenotypes similar to that of the *35S-IAA28-1* and *P$_{CsVMV}$-IAA28m* transgenic plants (Figures 5 and 6), such as fewer leaves and slender and uneven leaf blades with downward curled leaf margins (Figure 9A). In agreement with the fewer-leaf phenotype, higher levels of *CUC3* and *LOB* mRNAs were also detected in *IAA28m/miR847-8* line 2 plants (Figure 9C). Nevertheless, the overexpression of the cleavage-resistant form of *IAA28m* in *35S-miR$_{159}$847-8* mostly rescued its abnormal development morphologies in most of the tested auxin response genes, indicating that the overexpression of miR847 resulting in the cleavage of *IAA28* mRNA contributed to the abnormal phenotypes of *35S-miR$_{159}$847* plants and that miR847/IAA28 functions as an important module in the auxin signaling pathway, implicating miR847/IAA28 in the regulation of cell competence, thereby determining the duration of cell proliferation and lateral organ development in Arabidopsis.

DISCUSSION

miR847-Mediated *IAA28* mRNA Cleavage in Vivo

In both plants and animals, some *MIRNA* families are highly conserved through hundreds of millions of years (Axtell and Bartel, 2005; Grimson et al., 2008; Fahlgren et al., 2010). The miR847 sequence was identified by deep sequencing in Arabidopsis and *Arabidopsis lyrata*, but not in *Capsella rubella*, a species closely related to Arabidopsis within the Brassicaceae family (Rajagopalan et al., 2006; Fahlgren et al., 2010; Ma et al., 2010). *A. lyrata* and *C. rubella* diverged from Arabidopsis ~10 and ~20 million years ago, respectively (Koch et al., 2000; Wright et al., 2002; Fahlgren et al., 2010). Thus, the miR847-coding gene (*MIR847*) should be an orthologous conserved locus in the Arabidopsis lineage and one of the newer *MIRNA* genes (Fahlgren et al., 2010), which are generally expressed from single genes at low levels or primarily in specific cells or growth conditions (Rajagopalan et al., 2006). Using coexpression in *N. benthamiana*, we demonstrate here that miR847 targets *IAA28* mRNA for cleavage in vivo at the *IAA28*/miR847 complementary region and that the disruption of the base-pairing region compromised cleavage. In Arabidopsis, both miR847 and *IAA28* mRNA exhibit similar expression patterns and striking cell type specificity. *IAA28* mRNA cleavage might be developmentally regulated in response to auxin in Arabidopsis because the accumulation of miR847, which was undetectable under normal growth conditions, increased with decreasing *IAA28* mRNA levels upon auxin treatment. *IAA28* mRNA encodes an

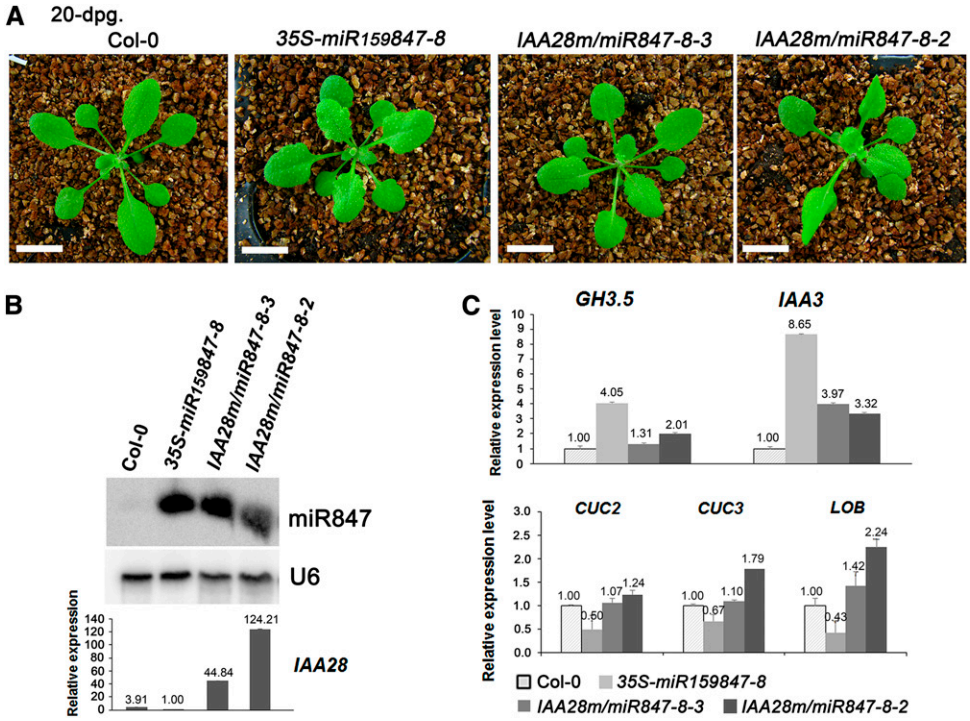

Figure 9. Phenotypes of Plants Overexpressing the Cleavage-Resistant Form of *IAA28* mRNA in *35S-miR$_{159}$847-8* Transgenic Lines.

(A) Phenotypes of Col-0, *35S-miR$_{159}$847-8*, and *IAA28m/miR847-8* plants. Bars = 10 mm.

(B) Expression of miR847 and *IAA28* mRNA in 10-d-old seedlings of Col-0, *35S-miR$_{159}$847-8*, and *IAA28m/miR847-8* plants. RNA gel blotting and qRT-PCR were done as described in Figure 2. The value of *IAA28* mRNA in *35S-miR$_{159}$847-8* was arbitrarily designated as 1. Error bars represent SD for three replicates.

(C) Expression of *GH3.5*, *IAA3*, *CUC2*, *CUC3*, and *LOB* mRNAs in 10-d-old seedlings of Col-0, *35S-miR$_{159}$847-8*, and *IAA28m/miR847-8* (lines 2 and 3) plants. qRT-PCR was done as described in Figure 7. The value of each mRNA in Col-0 was arbitrarily designated as 1. Error bars represent SD for three replicates.

Aux/IAA repressor protein that is targeted for degradation through the proteasome. This study extends our knowledge of the sensitization of auxin signaling to *IAA28* mRNA levels, which, together with targeted IAA28 degradation, ensures a robust signal derepression. This result is in agreement with the previous corollary that unstable mRNAs are less likely to encode stable proteins, such as NAC1, which is targeted by the SINAT5 E3 ligase for the 26S proteasome through polyubiquitination (Xie et al., 2002); its mRNA is also targeted by miR164-mediated cleavage (Guo et al., 2005).

miR847 Positively Regulates Lateral Root Development by Derepressing the IAA28-Dependent Auxin Signaling Cascade

The plant hormone auxin plays an important role in lateral root initiation. IAA28 is a negative regulator of auxin signaling during lateral root development (Rogg et al., 2001), which functions by regulating the expression of the transcription factor gene *GATA23* in the basal meristem region (De Rybel et al., 2010). In plants overexpressing miR847 or in mutant plants with knocked out *IAA28* gene expression, the downregulation of *IAA28* mRNA produced more lateral roots, correlated with the increased expression of *GATA23* mRNA, compared with the wild-type Col-0. The transcription factor *NAC1* mRNA also positively transduces the auxin signal leading to lateral root emergence (Xie et al., 2000), and miR164 negatively regulates *NAC1* mRNA and lateral root development in response to auxin treatment (Guo et al., 2005). However, increased auxin signaling through the miR847-mediated downregulation of *IAA28* likely did not obviously affect miR164/*NAC1* mRNA expression. Indeed, the *35S-miR$_{159}$847-8* line, which highly expressed *GATA23* mRNA, not only developed lateral roots earlier but also exhibited prolonged production of lateral roots in the basal meristem region compared with Col-0. By contrast, increased *NAC1* mRNA levels promoted lateral root production, which was mostly observed near the hypocotyl/root junction (Guo et al., 2005). Thus, our data suggest that miR847 positively regulates lateral root development by derepressing the IAA28-dependent repression of *GATA23* expression during the auxin response.

miR847 Positively Regulates Aerial Lateral Organ Development by Derepressing the IAA28-Dependent Auxin Signaling Cascade

In addition to greater lateral root development, overexpressing miR847 or knockout of *IAA28* also altered the development of the aerial portion. We have provided several lines of evidence

demonstrating that miR847 functions as a positive regulator of auxin-mediated lateral organ development in the aerial portion by cleaving *IAA28* mRNA. (1) Plants overexpressing *IAA28* mRNA produced long hypocotyls and fewer rosette leaves, resembling the gain-of-function *iaa28-1* mutant. (2) Plants with high miR847 production accumulated lower levels of *IAA28* mRNA and produced short hypocotyls and more rosette leaves, resembling the knockout *iaa28-ko* mutant. (3) Overexpressing cleavage-resistant *IAA28m* in plants with high levels of miR847 restored the normal growth of the hypocotyl and the number of rosette leaves. (4) In addition to the hypocotyl and leaf numbers, the leaf size and morphology were opposite between the plants overexpressing miR847 and those overexpressing *IAA28* mRNA. In every case, there is a strict inverse correlation between changes in the miR847 levels and changes in both the *IAA28* mRNA levels and leaf numbers and morphology.

The roles of auxin signaling mediators have been demonstrated in diverse development processes, including hypocotyl growth (Hagen and Guilfoyle, 2002). The Arabidopsis *GH3.5* gene (*WES1*) encodes an auxin-conjugating enzyme that functions in hypocotyl growth (Park et al., 2007). Both *GH3.5* and *IAA3* expression decreased in the long-hypocotyl *35S-IAA28* plants but increased in *35S-miR$_{159}$847* plants, which had short hypocotyls. *IAA3* is a negative regulator of auxin signaling (Tian et al., 2002). Our findings, together with the observation that gain-of-function mutations in *IAA3* cause short hypocotyls and do not affect *IAA28* expression (Tian et al., 2002), suggest that IAA28 probably acts upstream of IAA3 and that a reduction in *IAA28* expression stimulates an increase in the expression of other auxin signaling repressors, such as *IAA3*. However, increased *IAA3* expression in *35S-miR$_{159}$847* plants did not affect the expression of *GH3.5* mRNA. Thus, our data suggest that an auxin signaling pathway, miR847-IAA28-GH3.5, and its regulation function in hypocotyl development in Arabidopsis.

The overexpression of miR847 or knockout of *IAA28* in plants also produces more rosette leaves. The initiation of lateral organs from the SAM is associated with the formation of boundaries that separate the primordia from surrounding tissue (Aida and Tasaka, 2006; Rast and Simon, 2008). *CUC2* and *CUC3* mRNAs are expressed at the boundary between the shoot meristem and leaf primordia (Hibara et al., 2006). The region that produces leaf primordium in the SAM requires high auxin concentrations to restrict the expression of *CUC* genes, which are required for the activation of *Shoot Meristemless*, which maintains the meristematic fate in the SAM (Berleth et al., 2004; Laufs et al., 2004; Inukai et al., 2005; Shani et al., 2006; Okushima et al., 2007; Rast and Simon, 2008). *LOB* is also expressed in the boundary region at the base of all lateral organs and mediates responses to auxin (Husbands et al., 2007). The increased rosette leaf numbers in the *35S-miR$_{159}$847* and *iaa28-ko* plants decreased the expression of *CUC* family and *LOB* genes, suggesting that the miR847-mediated downregulation of *IAA28* results in auxin responsiveness in the SAM, promoting leaf primordia formation, consequently impeding the vegetative SAMs from being transformed into inflorescence meristems and generating floral meristems that produce floral organs. This notion explains the delayed florescence in *35S-miR$_{159}$847* plants. By contrast, the *35S-IAA28* plants develop early inflorescences due to the more stable IAA28 protein depressing the auxin signaling pathway. In Arabidopsis, the redundant functions of the *CUC1*, *CUC2*, and *CUC3* genes regulate embryonic shoot meristem formation and cotyledon boundary specification (Mallory et al., 2004; Shani et al., 2006). *CUC3* and *CUC2* are responsible for the axillary shoot formation and boundary specification of various postembryonic shoot organs, whereas the contribution of *CUC1* and *CUC2* during embryogenesis is greater than that of *CUC3* (Hibara et al., 2006). There was no obvious developmental defect observed in embryogenesis in the *35S-miR$_{159}$847* plants. Taken together, our data suggest that miR847-IAA28-mediated auxin signaling affects the formation of postembryonic shoot meristems, but not of the embryonic meristem, by regulating *LOB* and *CUC* family genes.

miR847 Positively Regulates Meristematic Competence and Cell Proliferation by Derepressing the IAA28-Dependent Auxin Signaling Cascade

The determination of organ size is a fundamental aspect of growth and development. The cell cycle genes *CYCD3;1* and *CYCB1;1* determine the leaf cell number and are regulated by auxin (Casimiro et al., 2001; Oakenfull et al., 2002; Dewitte et al., 2003). The finding that the expression of both *CYCD3;1* and *CYCB1;1* increases in *35S-miR$_{159}$847* and *iaa28-ko* plants, together with the observation that both *MIR847* and *IAA28* are expressed in the marginal meristems of rosette leaves where cells maintain meristematic competence, prolonging the growth of 8th to 10th rosette leaves in *35S-miR$_{159}$847* and *iaa28-ko* plants before floral organ development, indicate that miR847 plays a positive regulatory role in cell division-related leaf development. The transition from vegetative SAMs to inflorescence meristems and, finally, to floral organ development is mediated by a complex network of genetic pathways that regulate flowering in response to environmental and developmental signals (Liu et al., 2009). The regulation of auxin flux in response to endogenous cues in this transition is likely strong and restricts miR847-related regulation. The growth of rosette leaves after floral organ development was restricted in all plant genotypes, including wild-type Col-0, *35S-miR$_{159}$847*, and *iaa28-ko* mutant as well as *35S-IAA28* plants. Although more leaf primordia likely formed before inflorescence meristem formation in *35S-miR$_{159}$847* and *iaa28-ko* plants, the growth of the late-stage rosette leaves after visible floral growth was also restricted. Nonetheless, the effect of miR847 on cell division-related leaf development before floral development is demonstrated. Our results, together with the fact that the *35S-IAA28* and *P$_{CsVMV}$-IAA28m* plants present small leaves and that miR847 and IAA28 have opposite effects on cell proliferation during the formation of calli by tissue culture, suggest that miR847 positively regulates meristematic competence and cell proliferation by derepressing the IAA28-dependent auxin signaling cascade.

In summary, we identify a nonconserved miR847 that is not detected under normal conditions and is induced upon auxin treatment. *IAA28* mRNA, encoding an Aux/IAA repressor protein, is targeted by miR847 for cleavage. The striking cell type

specificity of both miR847 and *IAA28* as well as the induction of miR847 coincide with decreased *IAA28* mRNA levels upon auxin treatment, which was not observed in *tir1-1* and *axr1-3* mutants. These findings suggest that the auxin-dependent induction of miR847 is positively regulated in response to developmental switches to regulate the extent of cell competence, thereby determining the duration of cell proliferation and lateral organ growth through degradation of the transcript encoding the Aux/IAA28 repressor protein, which is concurrent with its degradation by the proteasomes and followed by the activation of relevant auxin-responsive molecular components.

METHODS

Plant Materials and Growth Conditions

Arabidopsis thaliana ecotypes Col-0 and Ws were used as the wild-type lines. The *tir1-1* and *axr1-3* mutant seeds (gifts from Mark Estelle), all transgenic plants, and knockout mutant *iaa28-ko* (SALK_129988C) used in this study are in the Col-0 background, and the gain-of-function *iaa28-1* mutant is in the Ws background. Arabidopsis plants were grown under long-day conditions (16 h of light/8 h of dark) at 22°C.

Cloning, Constructs, and Plant Transformation

For the *MIR847-GUS* and *IAA28-GUS* constructs, the 2480-bp upstream sequence of the *MIR847* gene and the 2041-bp upstream sequence of the *IAA28* gene were amplified, and PCR products were cloned into T-vectors (Tiangen) using T4 DNA Ligase (Takara). After confirmation by sequencing, *MIR847* and *IAA28* promoter sequences were individually subcloned into the pCAMBIA1300-221 binary vectors fused to the *GUS* reporter gene. For 35S-MIR847 and 35S-IAA28 constructs, the 259-bp genomic sequence of the *MIR847* and *IAA28* coding sequences was amplified, and the PCR product was cloned into T-vectors and confirmed by sequencing. *MIR847* and *IAA28* gene sequences were individually subcloned into the pCAMBIA1300-221 binary vector under the control of the 35S promoter. These plasmids, *MIR847-GUS*, *IAA28-GUS*, *35S-MIR847*, and *35S-IAA28*, were individually introduced into Col-0 plants using *Agrobacterium tumefaciens* EHA105 (Hood et al., 1993), and transformants were selected on medium containing hygromycin (30 mg/mL).

For the 35S-miR$_{159}$847 construct, the miR847-containing artificial miRNA precursor was amplified with the Arabidopsis precursor miR159a sequence as a backbone as described previously (Niu et al., 2006). The forward and reverse primers contain the miR847* sequence (Supplemental Data Set 2) and the mature miR847 reverse complementary sequence, respectively. The resulting PCR fragment was cloned into T-vector and confirmed by sequencing, then subcloned into the pCAMBIA1300-221 binary vector under the control of the 35S promoter to generate 35S-miR$_{159}$847 for transformation.

For the cleavage-resistant P_{CsVMV}-*IAA28m* construct, *IAA28* genomic sequence was amplified from the wild-type Col-0 genome. Oligonucleotide-directed mutagenesis was introduced into the *IAA28* genomic fragment with two primers in opposite orientations, IAA28m5′ and IAA28m3′ (Supplemental Data Set 2), using the Site-Directed Mutagenesis Kit (New England Biolabs) according to the manual. After it was confirmed by sequencing, the *IAA28m* sequence was subcloned into the pCAMBIA1300-221 binary vector, which contains the CsVMV promoter (Li et al., 2010), giving P_{CsVMV}-*IAA28m*, and retransformed to *35S-miR$_{159}$847* line 8 plants using Agrobacterium EHA105. Transformants were selected on medium containing 30 mg/L hygromycin and 50 mg/L kanamycin.

All primer sequences are listed in Supplemental Data Set 2.

GUS Staining

Seedlings, leaves, and flowers of *MIR847-GUS* and *IAA28-GUS* transgenic plants were stained in a GUS staining solution [2 mM 5-bromo-4-chloro-3-indolyl-β-D-glucuronic acid, 100 mM Na_3PO_4 buffer, 2 mM each $K_3Fe(CN)_6$/$K_4Fe(CN)_6$, and 0.5% Triton X-100] and incubated at 37°C overnight. After GUS staining, chlorophyll was removed using 70% ethanol.

5′ RLM-RACE Assay

The 5′ RACE assay was performed by using the First Choice RLM-RACE kit (Ambion). Portions (2 μg) of total RNAs were collected for direct ligation to the 5′ RACE RNA adapter, and subsequent steps were performed according to the manufacturer's directions. PCR fragments obtained from 5′ RACE were inserted into the pGEM-T vector (Tiangen), and individual clones were selected for DNA sequencing.

Agrobacterium Infiltration

The *35S-miR$_{159}$847*, P_{CsVMV}-*IAA28m*, *35S-IAA28*, and pCAMBIA1300-221 (control vector) constructs were transformed into the EHA105 strain of Agrobacterium by electroporation and selected on Luria-Bertani medium containing kanamycin at 50 mg/L and rifampicin at 10 mg/L. For Agrobacterium infiltration experiments, equal volumes of an Agrobacterium culture containing *35S-IAA28* or P_{CsVMV}-*IAA28m* (OD_{600} = 0.5) with the *35S-miR$_{159}$847* or pCAMBIA1300-221 (OD_{600} = 1.5) were mixed before infiltration and coinfiltrated into leaves of *Nicotiana benthamiana*.

NAA Treatment

Wild-type Col-0 and *tir1-1* and *axr1-3* mutants were cultured in Murashige and Skoog (MS) medium with 30% sucrose for 10 d, then placed in solutions with 10 or 20 μM NAA. Seedling samples were collected at various times for RNA analysis.

RNA Gel Blotting

Total RNA was extracted from plant tissue using the TRIzol reagent (Invitrogen). For low molecular weight RNA gel blots, 80 or 60 μg of total RNA was separated by electrophoresis on 17% PAGE gels and electrically transferred to nylon N+ membrane. [γ-^{32}P]ATP-labeled specific oligonucleotide probe sequences were used. For high molecular weight RNA gel blots, 30 μg of total RNA was separated on 1.2% agarose gels containing 6% formaldehyde and transferred to nylon N+ membrane. DNA probes were labeled with [α-^{32}P]dCTP using the Rediprime II system (Amersham).

RNA Isolation and qRT-PCR Analysis

Total RNA was extracted from Arabidopsis seedlings and rosette leaves using TRIzol reagent (Invitrogen). DNA residues of total RNA were removed using DNase I (Takara). Total RNA was then reverse transcribed into cDNA using SuperScript III reverse transcriptase (Promega). qRT-PCR analysis was performed with a 1000 series Thermal Cycling Platform (Bio-Rad) using GoTaq qPCR Master Mix (Promega). The primers used for qRT-PCR are listed in Supplemental Data Set 2. At least three biological replicates and three technical replicates within an experiment for each sample were performed.

Histological Analysis

Leaves and seedlings were fixed in 90% ethanol and 10% acetic acid for 1 h and gradually hydrated using serial dilutions of ethanol solutions (90, 70, 50, and 30%). The samples were washed with distilled water and then

dipped in 16.1 M chloral hydrate in glycerol:water (1:2, v/v) solution for transparentizing. The transparentized tissues were observed using an HC/DMR microscope (Leica) equipped with Nomarski optics. The middle part of the leaf was used for microscopic observation.

Leaf Explant Culture

Rosette leaves of 2-week-old Col-0, *35S-miR$_{159}$847*, *35S-IAA28*, and *P$_{CsVMV}$-IAA28m* transgenic plants, and the *iaa28-ko* mutant were excised. The explants were cultured on callus induction medium in the dark at 22°C. The callus induction medium used was MS medium containing 100 ng/L 2,4-D and 100 ng/L 6-BA (Hu et al., 2000). Photograph was taken at 7 d without changing the medium.

Bioinformatics and Statistical Analysis

Putative targets for miR847 were predicted through computational approaches at http://omicslab.genetics.ac.cn/psRobot/ (Wu et al., 2012). Statistical analysis was performed using Excel at http://www.microsoft.com/. Data shown are means ± SD.

Accession Numbers

Sequence data from this article can be found in the GenBank/EMBL libraries under the following accession numbers: AT1G07051 (*MIR847A*), AT5G25890 (*IAA28*), AT5G60890 (*ATR1*), AT3G62980 (*TIR1*), AT1G05180 (*AXR1*), AT5G26930 (*GATA23*), AT1G56010 (*NAC1*), AT4G27260 (*GH3.5*), AT4G37390 (*GH3.2*), AT1G04240 (*IAA3*), AT3G15170 (*CUC1*), AT5G53950 (*CUC2*), AT1G76420 (*CUC3*), AT5G63090 (*LOB*), AT4G34160 (*CYCD3;1*), AT4G37490 (*CYCB1;1*), and AT4G14560 (*IAA1*).

Supplemental Data

Supplemental Figure 1. Expression pattern of *GUS* transcript in *IAA28-GUS* and *MIR847-GUS* transgenic plants upon auxin treatment.

Supplemental Figure 2. Lateral root development in gain-of-function mutant *iaa28-1* and wild type control Wassilewskija.

Supplemental Figure 3. Phenotypes of transgenic plants overexpressing miR847 or *IAA28*, and *IAA28* lost-of-function and gain-of-function mutants.

Supplemental Data Set 1. Predicted putative targets for miR847 through computational approaches (Wu et al., 2012).

Supplemental Data Set 2. List of primers and DNA oligos used in this study.

ACKNOWLEDGMENTS

We thank Bonnie Bartel for the *iaa28-1* mutant seeds, Qi Xie for the *iaa28-ko* (SALK_129988C from the ABRC) mutant seeds and the wild-type Arabidopsis Ws seeds, and Oliver Yu for CsVMV promoter-containing plasmid. We thank Xiang-Feng He and Meng Liu for the 35S-miR$_{159}$847 construct. This research was supported by the National Science Foundation of China (Grant 31030009) and the Ministry of Science and Technology (Grant 2011CB100703).

AUTHOR CONTRIBUTIONS

J.-J.W. and H.-S.G. designed the research. J.-J.W. performed the research. J.-J.W. and H.-S.G. wrote the article.

Received February 2, 2015; revised February 20, 2015; accepted March 5, 2015; published March 20, 2015.

REFERENCES

Achard, P., Herr, A., Baulcombe, D.C., and Harberd, N.P. (2004). Modulation of floral development by a gibberellin-regulated microRNA. Development **131:** 3357–3365.

Aida, M., and Tasaka, M. (2006). Genetic control of shoot organ boundaries. Curr. Opin. Plant Biol. **9:** 72–77.

Aukerman, M.J., and Sakai, H. (2003). Regulation of flowering time and floral organ identity by a microRNA and its APETALA2-like target genes. Plant Cell **15:** 2730–2741.

Axtell, M.J., and Bartel, D.P. (2005). Antiquity of microRNAs and their targets in land plants. Plant Cell **17:** 1658–1673.

Baker, C.C., Sieber, P., Wellmer, F., and Meyerowitz, E.M. (2005). The early extra petals1 mutant uncovers a role for microRNA miR164c in regulating petal number in Arabidopsis. Curr. Biol. **15:** 303–315.

Berleth, T., Krogan, N.T., and Scarpella, E. (2004). Auxin signals—Turning genes on and turning cells around. Curr. Opin. Plant Biol. **7:** 553–563.

Carthew, R.W., and Sontheimer, E.J. (2009). Origins and mechanisms of miRNAs and siRNAs. Cell **136:** 642–655.

Casimiro, I., Marchant, A., Bhalerao, R.P., Beeckman, T., Dhooge, S., Swarup, R., Graham, N., Inzé, D., Sandberg, G., Casero, P.J., and Bennett, M. (2001). Auxin transport promotes *Arabidopsis* lateral root initiation. Plant Cell **13:** 843–852.

Chen, X. (2004). A microRNA as a translational repressor of APETALA2 in Arabidopsis flower development. Science **303:** 2022–2025.

Chiou, T.J., Aung, K., Lin, S.I., Wu, C.C., Chiang, S.F., and Su, C.L. (2006). Regulation of phosphate homeostasis by microRNA in *Arabidopsis*. Plant Cell **18:** 412–421.

De Rybel, B., et al. (2010). A novel aux/IAA28 signaling cascade activates GATA23-dependent specification of lateral root founder cell identity. Curr. Biol. **20:** 1697–1706.

Dewitte, W., Riou-Khamlichi, C., Scofield, S., Healy, J.M., Jacqmard, A., Kilby, N.J., and Murray, J.A. (2003). Altered cell cycle distribution, hyperplasia, and inhibited differentiation in *Arabidopsis* caused by the D-type cyclin CYCD3. Plant Cell **15:** 79–92.

Dharmasiri, N., Dharmasiri, S., and Estelle, M. (2005a). The F-box protein TIR1 is an auxin receptor. Nature **435:** 441–445.

Dharmasiri, N., Dharmasiri, S., Weijers, D., Lechner, E., Yamada, M., Hobbie, L., Ehrismann, J.S., Jürgens, G., and Estelle, M. (2005b). Plant development is regulated by a family of auxin receptor F box proteins. Dev. Cell **9:** 109–119.

Donnelly, P.M., Bonetta, D., Tsukaya, H., Dengler, R.E., and Dengler, N.G. (1999). Cell cycling and cell enlargement in developing leaves of Arabidopsis. Dev. Biol. **215:** 407–419.

Dreher, K.A., Brown, J., Saw, R.E., and Callis, J. (2006). The *Arabidopsis* Aux/IAA protein family has diversified in degradation and auxin responsiveness. Plant Cell **18:** 699–714.

Duan, C.G., Wang, C.H., Fang, R.X., and Guo, H.S. (2008). Artificial microRNAs highly accessible to targets confer efficient virus resistance in plants. J. Virol. **82:** 11084–11095.

Fahlgren, N., Jogdeo, S., Kasschau, K.D., Sullivan, C.M., Chapman, E.J., Laubinger, S., Smith, L.M., Dasenko, M., Givan, S.A., Weigel, D., and Carrington, J.C. (2010). MicroRNA gene evolution in *Arabidopsis lyrata* and *Arabidopsis thaliana*. Plant Cell **22:** 1074–1089.

Ferreira, P., Hemerly, A., de Almeida Engler, J., Bergounioux, C., Burssens, S., Van Montagu, M., Engler, G., and Inzé, D. (1994a).

Three discrete classes of Arabidopsis cyclins are expressed during different intervals of the cell cycle. Proc. Natl. Acad. Sci. USA **91:** 11313–11317.

Ferreira, P.C., Hemerly, A.S., Engler, J.D., van Montagu, M., Engler, G., and Inzé, D. (1994b). Developmental expression of the *Arabidopsis* cyclin gene cyc1At. Plant Cell **6:** 1763–1774.

Fujii, H., Chiou, T.J., Lin, S.I., Aung, K., and Zhu, J.K. (2005). A miRNA involved in phosphate-starvation response in Arabidopsis. Curr. Biol. **15:** 2038–2043.

Grimson, A., Srivastava, M., Fahey, B., Woodcroft, B.J., Chiang, H.R., King, N., Degnan, B.M., Rokhsar, D.S., and Bartel, D.P. (2008). Early origins and evolution of microRNAs and Piwi-interacting RNAs in animals. Nature **455:** 1193–1197.

Guilfoyle, T.J., and Hagen, G. (2007). Auxin response factors. Curr. Opin. Plant Biol. **10:** 453–460.

Guo, H.S., Xie, Q., Fei, J.F., and Chua, N.H. (2005). MicroRNA directs mRNA cleavage of the transcription factor NAC1 to downregulate auxin signals for *Arabidopsis* lateral root development. Plant Cell **17:** 1376–1386.

Gutierrez, L., Bussell, J.D., Pacurar, D.I., Schwambach, J., Pacurar, M., and Bellini, C. (2009). Phenotypic plasticity of adventitious rooting in *Arabidopsis* is controlled by complex regulation of AUXIN RESPONSE FACTOR transcripts and microRNA abundance. Plant Cell **21:** 3119–3132.

Hagen, G., and Guilfoyle, T. (2002). Auxin-responsive gene expression: Genes, promoters and regulatory factors. Plant Mol. Biol. **49:** 373–385.

Hibara, K., Karim, M.R., Takada, S., Taoka, K., Furutani, M., Aida, M., and Tasaka, M. (2006). *Arabidopsis* CUP-SHAPED COTYLEDON3 regulates postembryonic shoot meristem and organ boundary formation. Plant Cell **18:** 2946–2957.

Hood, E.E., Gelvin, S.B., Melchers, L.S., and Hoekema, A. (1993). New *Agrobacterium* helper plasmids for gene transfer to plants. Transgenic Res. **2:** 208–218.

Hu, J.Y., Zhou, Y., He, F., Dong, X., Liu, L.Y., Coupland, G., Turck, F., and de Meaux, J. (2014). miR824-regulated AGAMOUS-LIKE16 contributes to flowering time repression in *Arabidopsis*. Plant Cell **26:** 2024–2037.

Hu, Y., Bao, F., and Li, J. (2000). Promotive effect of brassinosteroids on cell division involves a distinct CycD3-induction pathway in Arabidopsis. Plant J. **24:** 693–701.

Husbands, A., Bell, E.M., Shuai, B., Smith, H.M., and Springer, P.S. (2007). LATERAL ORGAN BOUNDARIES defines a new family of DNA-binding transcription factors and can interact with specific bHLH proteins. Nucleic Acids Res. **35:** 6663–6671.

Inukai, Y., Sakamoto, T., Ueguchi-Tanaka, M., Shibata, Y., Gomi, K., Umemura, I., Hasegawa, Y., Ashikari, M., Kitano, H., and Matsuoka, M. (2005). Crown rootless1, which is essential for crown root formation in rice, is a target of an AUXIN RESPONSE FACTOR in auxin signaling. Plant Cell **17:** 1387–1396.

Jones-Rhoades, M.W., and Bartel, D.P. (2004). Computational identification of plant microRNAs and their targets, including a stress-induced miRNA. Mol. Cell **14:** 787–799.

Jones-Rhoades, M.W., Bartel, D.P., and Bartel, B. (2006). MicroRNAS and their regulatory roles in plants. Annu. Rev. Plant Biol. **57:** 19–53.

Juarez, M.T., Kui, J.S., Thomas, J., Heller, B.A., and Timmermans, M.C. (2004). MicroRNA-mediated repression of rolled leaf1 specifies maize leaf polarity. Nature **428:** 84–88.

Kim, J.J., Lee, J.H., Kim, W., Jung, H.S., Huijser, P., and Ahn, J.H. (2012). The microRNA156-SQUAMOSA PROMOTER BINDING PROTEIN-LIKE3 module regulates ambient temperature-responsive flowering via FLOWERING LOCUS T in Arabidopsis. Plant Physiol. **159:** 461–478.

Koch, M.A., Haubold, B., and Mitchell-Olds, T. (2000). Comparative evolutionary analysis of chalcone synthase and alcohol dehydrogenase loci in Arabidopsis, Arabis, and related genera (Brassicaceae). Mol. Biol. Evol. **17:** 1483–1498.

Kruszka, K., Pieczynski, M., Windels, D., Bielewicz, D., Jarmolowski, A., Szweykowska-Kulinska, Z., and Vazquez, F. (2012). Role of microRNAs and other sRNAs of plants in their changing environments. J. Plant Physiol. **169:** 1664–1672.

Laufs, P., Peaucelle, A., Morin, H., and Traas, J. (2004). MicroRNA regulation of the CUC genes is required for boundary size control in Arabidopsis meristems. Development **131:** 4311–4322.

Li, H., Deng, Y., Wu, T., Subramanian, S., and Yu, O. (2010). Misexpression of miR482, miR1512, and miR1515 increases soybean nodulation. Plant Physiol. **153:** 1759–1770.

Li, S., et al. (2013). MicroRNAs inhibit the translation of target mRNAs on the endoplasmic reticulum in Arabidopsis. Cell **153:** 562–574.

Liu, C., Thong, Z., and Yu, H. (2009). Coming into bloom: The specification of floral meristems. Development **136:** 3379–3391.

Liu, X., Huang, J., Wang, Y., Khanna, K., Xie, Z., Owen, H.A., and Zhao, D. (2010). The role of floral organs in carpels, an Arabidopsis loss-of-function mutation in microRNA160a, in organogenesis and the mechanism regulating its expression. Plant J. **62:** 416–428.

Ma, Z., Coruh, C., and Axtell, M.J. (2010). *Arabidopsis lyrata* small RNAs: Transient MIRNA and small interfering RNA loci within the *Arabidopsis* genus. Plant Cell **22:** 1090–1103.

Mallory, A.C., Bartel, D.P., and Bartel, B. (2005). MicroRNA-directed regulation of *Arabidopsis* AUXIN RESPONSE FACTOR17 is essential for proper development and modulates expression of early auxin response genes. Plant Cell **17:** 1360–1375.

Mallory, A.C., Dugas, D.V., Bartel, D.P., and Bartel, B. (2004). MicroRNA regulation of NAC-domain targets is required for proper formation and separation of adjacent embryonic, vegetative, and floral organs. Curr. Biol. **14:** 1035–1046.

Marin, E., Jouannet, V., Herz, A., Lokerse, A.S., Weijers, D., Vaucheret, H., Nussaume, L., Crespi, M.D., and Maizel, A. (2010). miR390, *Arabidopsis* TAS3 tasiRNAs, and their AUXIN RESPONSE FACTOR targets define an autoregulatory network quantitatively regulating lateral root growth. Plant Cell **22:** 1104–1117.

Navarro, L., Dunoyer, P., Jay, F., Arnold, B., Dharmasiri, N., Estelle, M., Voinnet, O., and Jones, J.D. (2006). A plant miRNA contributes to antibacterial resistance by repressing auxin signaling. Science **312:** 436–439.

Niu, Q.W., Lin, S.S., Reyes, J.L., Chen, K.C., Wu, H.W., Yeh, S.D., and Chua, N.H. (2006). Expression of artificial microRNAs in transgenic Arabidopsis thaliana confers virus resistance. Nat. Biotechnol. **24:** 1420–1428.

Oakenfull, E.A., Riou-Khamlichi, C., and Murray, J.A.H. (2002). Plant D-type cyclins and the control of G1 progression. Philos. Trans. R. Soc. Lond. B Biol. Sci. **357:** 749–760.

Okushima, Y., Fukaki, H., Onoda, M., Theologis, A., and Tasaka, M. (2007). ARF7 and ARF19 regulate lateral root formation via direct activation of LBD/ASL genes in *Arabidopsis*. Plant Cell **19:** 118–130.

Palatnik, J.F., Allen, E., Wu, X., Schommer, C., Schwab, R., Carrington, J.C., and Weigel, D. (2003). Control of leaf morphogenesis by microRNAs. Nature **425:** 257–263.

Park, J.E., Seo, P.J., Lee, A.K., Jung, J.H., Kim, Y.S., and Park, C.M. (2007). An Arabidopsis GH3 gene, encoding an auxin-conjugating enzyme, mediates phytochrome B-regulated light signals in hypocotyl growth. Plant Cell Physiol. **48:** 1236–1241.

Park, W., Li, J., Song, R., Messing, J., and Chen, X. (2002). CARPEL FACTORY, a Dicer homolog, and HEN1, a novel protein, act in microRNA metabolism in *Arabidopsis thaliana*. Curr. Biol. **12:** 1484–1495.

Rajagopalan, R., Vaucheret, H., Trejo, J., and Bartel, D.P. (2006). A diverse and evolutionarily fluid set of microRNAs in *Arabidopsis thaliana*. Genes Dev. **20:** 3407–3425.

Ramos, J.A., Zenser, N., Leyser, O., and Callis, J. (2001). Rapid degradation of auxin/indoleacetic acid proteins requires conserved amino acids of domain II and is proteasome dependent. Plant Cell **13:** 2349–2360.

Rast, M.I., and Simon, R. (2008). The meristem-to-organ boundary: More than an extremity of anything. Curr. Opin. Genet. Dev. **18:** 287–294.

Reinhart, B.J., Weinstein, E.G., Rhoades, M.W., Bartel, B., and Bartel, D.P. (2002). MicroRNAs in plants. Genes Dev. **16:** 1616–1626.

Rhoades, M.W., Reinhart, B.J., Lim, L.P., Burge, C.B., Bartel, B., and Bartel, D.P. (2002). Prediction of plant microRNA targets. Cell **110:** 513–520.

Rogg, L.E., Lasswell, J., and Bartel, B. (2001). A gain-of-function mutation in IAA28 suppresses lateral root development. Plant Cell **13:** 465–480.

Schwab, R., Palatnik, J.F., Riester, M., Schommer, C., Schmid, M., and Weigel, D. (2005). Specific effects of microRNAs on the plant transcriptome. Dev. Cell **8:** 517–527.

Shani, E., Yanai, O., and Ori, N. (2006). The role of hormones in shoot apical meristem function. Curr. Opin. Plant Biol. **9:** 484–489.

Staswick, P.E., Serban, B., Rowe, M., Tiryaki, I., Maldonado, M.T., Maldonado, M.C., and Suza, W. (2005). Characterization of an *Arabidopsis* enzyme family that conjugates amino acids to indole-3-acetic acid. Plant Cell **17:** 616–627.

Sunkar, R., and Zhu, J.K. (2004). Novel and stress-regulated microRNAs and other small RNAs from *Arabidopsis*. Plant Cell **16:** 2001–2019.

Sunkar, R., Kapoor, A., and Zhu, J.K. (2006). Posttranscriptional induction of two Cu/Zn superoxide dismutase genes in *Arabidopsis* is mediated by downregulation of miR398 and important for oxidative stress tolerance. Plant Cell **18:** 2051–2065.

Tang, G., Reinhart, B.J., Bartel, D.P., and Zamore, P.D. (2003). A biochemical framework for RNA silencing in plants. Genes Dev. **17:** 49–63.

Tian, Q., Uhlir, N.J., and Reed, J.W. (2002). *Arabidopsis* SHY2/IAA3 inhibits auxin-regulated gene expression. Plant Cell **14:** 301–319.

Wang, J.W., Czech, B., and Weigel, D. (2009). miR156-regulated SPL transcription factors define an endogenous flowering pathway in *Arabidopsis thaliana*. Cell **138:** 738–749.

Wang, J.W., Wang, L.J., Mao, Y.B., Cai, W.J., Xue, H.W., and Chen, X.Y. (2005). Control of root cap formation by microRNA-targeted auxin response factors in *Arabidopsis*. Plant Cell **17:** 2204–2216.

Wright, S.I., Lauga, B., and Charlesworth, D. (2002). Rates and patterns of molecular evolution in inbred and outbred Arabidopsis. Mol. Biol. Evol. **19:** 1407–1420.

Wu, G., Park, M.Y., Conway, S.R., Wang, J.W., Weigel, D., and Poethig, R.S. (2009). The sequential action of miR156 and miR172 regulates developmental timing in Arabidopsis. Cell **138:** 750–759.

Wu, H.J., Ma, Y.K., Chen, T., Wang, M., and Wang, X.J. (2012). PsRobot: a web-based plant small RNA meta-analysis toolbox. Nucleic Acids Res. **40:** W22–W28.

Wu, M.F., Tian, Q., and Reed, J.W. (2006). Arabidopsis microRNA167 controls patterns of ARF6 and ARF8 expression, and regulates both female and male reproduction. Development **133:** 4211–4218.

Xie, Q., Frugis, G., Colgan, D., and Chua, N.H. (2000). Arabidopsis NAC1 transduces auxin signal downstream of TIR1 to promote lateral root development. Genes Dev. **14:** 3024–3036.

Xie, Q., Guo, H.S., Dallman, G., Fang, S., Weissman, A.M., and Chua, N.H. (2002). SINAT5 promotes ubiquitin-related degradation of NAC1 to attenuate auxin signals. Nature **419:** 167–170.

Xue, X.-Y., Zhao, B., Chao, L.-M., Chen, D.-Y., Cui, W.-R., Mao, Y.-B., Wang, L.-J., and Chen, X.-Y. (2014). Interaction between two timing microRNAs controls trichome distribution in Arabidopsis. PLoS Genet. **10:** e1004266.

Yoon, E.K., Yang, J.H., Lim, J., Kim, S.H., Kim, S.K., and Lee, W.S. (2010). Auxin regulation of the microRNA390-dependent transacting small interfering RNA pathway in Arabidopsis lateral root development. Nucleic Acids Res. **38:** 1382–1391.